Zeta Potential of Artificial and Natural Calcite in Aqueous Solution

Dawoud Al Mahrouqi[1, 2*], Jan Vinogradov[1, 3] and Matthew D. Jackson[1]

[1] Department of Earth Science and Engineering, Imperial College London, SW7 2AZ, United Kingdom

[2] Petroleum Development Oman, Muscat, P.O. Box 81, P.C. 113, Oman

[3] Now at the School of Engineering, University of Aberdeen, AB24 3UE, United Kingdom

[*] **Corresponding author. E-mail addresses:** d.al-mahrouqi12@imperial.ac.uk**,** dawoud.mahrouqi@gmail.com **(D. Al Mahrouqi).**

Abstract

Despite the broad range of interest and applications, controls on calcite surface charge in aqueous solution, especially at conditions relevant to natural systems, remain poorly understood. The primary data source to understand calcite surface charge comprises measurements of zeta potential. Here we collate and review previous measurements of zeta potential on natural and artificial calcite and carbonate as a resource for future studies, compare and contrast the results of these studies to determine key controls on zeta potential and where uncertainties remain, and report new measurements of zeta potential relevant to natural subsurface systems.

The results show that the potential determining ions (PDIs) for the carbonate mineral surface are the lattice ions Ca^{2+}, Mg^{2+} and CO_3^{2-}. The zeta potential is controlled by the

concentration-dependent adsorption of these ions within the Stern layer, primarily at the Outer Helmholtz Plane (OHP). Given this, the Iso-Electric Point (IEP) at which the zeta potential is zero should be expressed as pCa (or pMg). It should not be reported as pH, similar to most metal oxides.

The pH does not directly control the zeta potential. Varying the pH whilst holding pCa constant yields constant zeta potential. The pH affects the zeta potential only by moderating the equilibrium pCa for a given CO_2 partial pressure (pCO_2). Experimental studies that appear to yield a systematic relationship between pH and zeta potential are most likely observing the relationship between pCa and zeta potential, with pCa responding to the change in pH. New data presented here show a consistent linear relationship between equilibrium pH and equilibrium pCa or pMg irrespective of sample used or solution ionic strength. The surface charge of calcite is weakly dependent on pH, through protonation and deprotonation reactions that occur within a hydrolysis layer immediately adjacent to the mineral surface. The Point of Zero Charge (PZC) at which the surface charge is zero could be expressed as pH, but surface complexation models suggest the surface is negatively charged over the pH range 5.5-11.

Several studies have suggested that SO_4^{2-} is also a PDI for the calcite surface, but new data presented here indicate that the value of pSO_4 may affect zeta potential only by moderating the equilibrium pCa. Natural carbonate typically yields a more negative zeta potential than synthetic calcite, most likely due to the presence of impurities including clays, organic matter, apatite, anhydrite or quartz, that yield a more negative zeta potential than pure calcite. New data presented here show that apparently identical natural carbonates display differing zeta potential behavior, most likely due to the presence of small volumes of these impurities. It is important to ensure equilibrium, defined in terms of the concentration of PDIs, has been

reached prior to taking measurements. Inconsistent values of zeta potential obtained in some studies may reflect a lack of equilibration.

The data collated and reported here have broad application in engineering processes including the manufacture of paper and cement, the geologic storage of nuclear waste and CO_2, and the production of oil and gas.

Keywords

Zeta potential; Streaming potential; Calcite; Carbonate; Wettability alteration; Controlled salinity waterflooding

Contents of paper

1. Introduction

The properties of the calcite mineral surface and the interface between calcite and aqueous solution are of broad interest in many areas of science and engineering. Calcite is a common mineral, comprising approximately 4% of the Earth's crust, and surface reactions on calcite play an important role in many geochemical and environmental systems, as well as many areas of industry, including the manufacture of paper and cement (e.g. [5]), the geologic storage of nuclear waste and CO_2 (e.g. [30]), and the production of oil and gas (e.g. [9, 28, 86, 88]). However, despite the broad range of interest and applications, controls on calcite surface charge in aqueous solution, especially at conditions relevant to natural systems, remain poorly understood. Numerous papers have reported inconsistent or contradictory data and models, and there is still active debate over the relationship between calcite surface charge and electrolyte pH, the concentration of ions such as Ca^{2+}, Mg^{2+}, CO_3^{2-} and SO_4^{2-} in aqueous solution, the partial pressure of CO_2, the difference between natural and artificial calcite, and the role of dissolution and/or precipitation.

The focus of this paper is the zeta potential of artificial and natural calcite in aqueous solution. The zeta potential is an important measure of the electrical potential at the mineral surface, and the magnitude and sign of the zeta potential control the electrostatic interactions between the mineral surface and polar species in aqueous solution, between the mineral surface and other charged interfaces such as the water-air and water-oil interfaces, and between mineral particles in suspension including flocculation and dispersion. Measurements of zeta potential in low concentration solutions and at laboratory conditions are relatively straightforward, and most studies of the calcite mineral surface have reported measurements of zeta potential or the closely related property of electrophoretic mobility. Other approaches to determine surface charge, such as potentiometric titration, are challenging to apply in calcite because rapid dissolution kinetics and the buffering effect of carbonate ions in

123 solution can affect the results. Thus the primary data source to understand calcite surface
124 charge comprises measurements of zeta potential. Where relevant, we use the results of
125 spectroscopic, microscopic, surface diffraction, modelling and theoretical studies to help
126 explain experimentally determined values of zeta potential. However, a comprehensive
127 review of these studies is beyond the scope of the paper; a companion paper of comparable
128 length would be required to do justice to this work.

129 The aims of the paper are therefore threefold; (1) to collate and review previous
130 measurements of zeta potential on natural and artificial calcite and carbonate as a resource for
131 future studies, (2) to compare and contrast the results of these studies to determine key
132 controls on zeta potential and where uncertainties remain, and (3) to report new
133 measurements of zeta potential relevant to natural subsurface systems. There has been no
134 comprehensive review of zeta potential measurements in calcite and natural carbonate to
135 date, although Wolthers et al. [85] collated published zeta potential data to constrain their
136 new surface complexation model. Moreover, there are a lack of data which can be applied to
137 natural systems owing to the comparatively high ionic strength (typically >0.01M and often
138 >2M) and complex compositions (including Na^+, Ca^{2+}, Mg^{2+}, Cl^-, CO_3^{2-}, SO_4^{2-}) of natural
139 brines, compared to the simple, dilute aqueous solutions typically used in laboratory
140 experiments.

141 We report new data obtained using (intact) natural samples saturated with electrolytes
142 relevant to natural systems and an experimental methodology specifically designed to allow
143 this parameter space to be explored. Data obtained in this parameter space are still very
144 scarce, despite the broad range of interest. Our results demonstrate that apparently identical
145 natural carbonates can exhibit differing zeta potential behaviour, suggesting that small
146 variations in the type and content of impurities in the mineral lattice can significantly impact

147 the surface charge. However, the effect of the lattice ions Ca^{2+} and Mg^{2+} on the zeta potential
148 of a given carbonate is identical within experimental error. The presence of apparently
149 indifferent ions such as Na^{+} and Cl^{-} at the high concentrations typical of natural brines can
150 significantly shift the iso-electric point expressed as pCa and pMg. We demonstrate
151 experimentally that equilibrium pH is strongly correlated to equilibrium pCa and pMg, and
152 apparent trends in zeta potential with pH reflect trends in zeta potential with pCa and pMg.
153 Ca^{2+} and Mg^{2+} are the potential determining ions (PDIs) for the calcite surface. We provide
154 experimental evidence suggesting that SO_4^{2-}, which has previously been suggested as a PDI,
155 may not directly control the zeta potential of calcite; rather, varying pSO_4 causes variations in
156 pCa which can be correlated with observed changes on zeta potential. These new results have
157 broad application to subsurface engineering processes such as the geologic storage of nuclear
158 waste and CO_2, and the production of oil and gas.

159

160 **2. Zeta potential and the electrical double layer**

161 **2.1. The electrical double layer**

162 The immersion of a calcite mineral in aqueous solution leads to a separation of electrical
163 charge at the mineral-solution interface. An excess of charge at the mineral surface is
164 balanced by a region of equal but opposite charge in the adjacent solution, in an arrangement
165 often termed the electrical double layer (EDL; e.g. [25, 26]; see Fig. 1). The charge at the
166 mineral surface is balanced by a relative decrease in the concentration of co-ions (i.e. ions
167 with the same charge as the surface) and increase in the concentration of counter-ions (i.e.
168 ions with the opposite charge as the surface) in the adjacent solution. The region immediately
169 adjacent to the mineral surface is typically termed the Stern layer, and contains ions that are
170 attached to the mineral surface; the Stern layer may be further divided into the inner and outer

Helmoltz layers, defined by the inner and outer Helmoltz planes (the IHP and OHP shown in Fig. 1a; note the inner and outer Helmholtz layers and associated planes are also sometimes termed the inner and outer Stern layers and planes). The IHP defines the location of ions that closely approach the mineral surface and are attached to surface sites (Fig. 1a). The OHP defines the location of larger, typically hydrated ions that cannot enter the inner Helmholtz plane but which are nevertheless attached to the mineral surface [6].

In most cases, the charge in the Stern layer does not exactly balance the surface charge, giving rise to a 'diffuse' or 'Gouy-Chapman' layer that contains the remaining excess charge in the solution required to ensure electrical neutrality of the EDL (e.g. [43]). The difference between the Stern and diffuse layers is that the co- and counter-ions in the diffuse layer are not attached to the mineral surface. At low ionic strength ($\lesssim 0.1$M), the ion concentration in the diffuse layer decreases exponentially with distance from the OHP (Fig. 1a). The electrical potential corresponding to the charge distribution within the EDL decreases linearly with distance from the mineral surface through the Stern layer, although there may be a difference in gradient between the inner and outer Helmholtz layers, and exponentially with distance from the OHP through the diffuse layer, falling to zero in the uncharged solution (Fig. 1b).

2.2. Electrokinetic phenomena

Electrokinetic phenomena arise when there is a relative motion between the excess charge in the diffuse layer of the EDL and the charged surface [34]. It is typically assumed that the excess charge in the diffuse layer is mobile only beyond a plane termed the 'shear' or 'slip' plane that lies a small distance away from the OHP (Fig. 1). The zeta potential is the electrical potential at the shear plane. In some models of the EDL, it is assumed that the shear plane and the OHP are identical, in which case the zeta potential also represents the electrical potential at the OHP. Methods to determine the zeta potential make use of electrokinetic

phenomena, most typically (1) electrophoresis, which is the mobilisation of charged particles, relative to a stationary solution, under the influence of an applied electrical field, and (2) streaming potential, which is the potential difference that arises when a solution is moved relative to a stationary solid under the influence of an applied pressure gradient [15].

The electrophoretic method (termed here EPM) used to determine zeta potential is conducted on powdered samples suspended in the solution of interest. An electrical field E is applied across the suspension and the resulting velocity $\boldsymbol{v}_e$ of the charged particles is measured with respect to the solution. The velocity is then normalized by the electrical field to yield the electrophoretic mobility u_e, which is typically treated as an isotropic quantity that can be related to the zeta potential by the Helmholtz-Smoluchowski equation for electrophoresis [15]

$$u_e = \frac{\varepsilon\zeta}{\mu}, \quad (1)$$

where ε is the permittivity ($F \cdot m^{-1}$) and μ the viscosity ($Pa \cdot s$) of the solution. The zeta potential obtained using the EPM is an effective value across all the suspended particles; the zeta potential of individual particles (and, indeed, between the different faces of a given particle) may differ from the single value interpreted from EPM measurements.

The streaming potential method (termed here SPM) used to determine zeta potential is conducted using intact samples of porous materials, packed beds of particles, or surfaces through, or across, which the solution of interest is caused to flow. A pressure difference ΔP is applied across the sample and the resulting electrical potential difference ΔV is measured. The potential difference is then normalized by the pressure difference to yield the streaming potential coupling coefficient, which is typically treated as an isotropic quantity that can be related to the zeta potential by the Helmholtz-Smoluchowski equation for streaming potential (e.g. [17, 34, 52])

$$C = \frac{\varepsilon\zeta}{\sigma_s \mu}, \quad (2)$$

where σ_s is the electrical conductivity of the solution of interest ($S \cdot m^{-1}$). When streaming potential measurements are obtained in porous media, it may be necessary to use a version of equation (2) modified to account for the effect of enhanced electrical conductivity through the EDL (often termed surface electrical conductivity; [49])

$$C = \frac{\varepsilon\zeta}{\sigma_{ss} \mu F}, \quad (3)$$

where σ_{ss} is the electrical conductivity of the system saturated with the solution of interest and *F* is the so-called formation factor (dimensionless) which is defined as the ratio of the solution conductivity σ_s to the system conductivity σ_{ss} when surface electrical conductivity is negligible. The formation factor is typically measured on the system saturated with a concentrated solution with high electrical conductivity (e.g. [35, 40, 83]).

3. Development of surface charge on calcite in aqueous solution

3.1. Effect of pH

The development of surface charge on calcite in aqueous solution is still not fully understood [71, 79, 85]. In most metal oxides, charge development occurs when mineral surfaces sites are hydrated to form amphoteric groups >MeOH (where Me denotes a metal ion and > denotes the crystal lattice) and these react either with H^+ or OH^- ions according to (e.g. [61, 77])

$$>MeOH^0 + OH^- \Leftrightarrow >MeO^- + H_2O \quad (4)$$

$$>MeOH^0 + H^+ \Leftrightarrow >MeOH_2^+ \quad (5)$$

The relative abundance of negatively and positively charged surface sites depends on the relative concentration of H^+ and OH^- in solution; these ions behave as 'potential determining ions' (PDIs) for the surface. Consequently, the net surface charge depends on the solution pH. It is therefore common to see surface charge and/or zeta potential plotted as a function of pH, with the surface charge and/or zeta potential becoming more negative as the pH increases and the deprotonation reaction (4) is favoured, and more positive as the pH decreases and the protonation reaction (5) is favoured (e.g. [13, 32]). When the number of positively and negatively charged surface sites exactly balances, a surface charge of zero is observed and the corresponding pH is termed the 'point of zero charge' (PZC). A zeta potential of zero may also be observed and the corresponding pH is termed the 'iso-electric-point' (IEP) (e.g. [34]). The IEP and PZC may not coincide, for reasons discussed in more detail in the next section.

The surface of calcite differs from the metal oxides in several important respects. First, the mineral is soluble in aqueous solution and the lattice ions Ca^{2+} and CO_3^{2-} can be released into solution or deposited on the surface depending upon the solution pH [66, 75]. Second, atmospheric CO_2 in open system experiments can dissolve into solution, affecting the pH and the equilibrium concentrations of Ca^{2+}, CO_3^{2-} and HCO_3^- (e.g. [18]). Third, the hydrated calcite surface contains protonated anion surface sites $>CO_3H^0$ as well as hydroxylated cation sites $>CaOH^0$ (e.g. [57, 79]). Evidence to support the presence of these sites has been provided by X-ray photoelectron spectroscopic (XPS) and infrared (IR) spectroscopic measurements [56, 72, 73]. The protonation and deprotonation reactions at these surface sites, and therefore the relative abundance of positively and negatively charged sites on the mineral surface, is pH dependent according to the following reactions (e.g. [29, 57, 79])

$$>CaOH^0 + OH^- \Leftrightarrow >CaO^- + H_2O \quad (6)$$

$$>CO_3H^0 + OH^- \Leftrightarrow >CO_3^- + H_2O \quad (7)$$

264 $>CaOH^0 + H^+ \Leftrightarrow >CaOH_2^+$ (8)

265 Thus it would be expected that the surface charge, and hence the zeta potential, of calcite in
266 aqueous solution are both determined by the pH, with H^+ and OH^- behaving as the PDIs.
267 Numerous studies have determined the variation in zeta potential with pH for a variety of
268 calcite types and solution compositions (e.g. Fig. 2).

269 However, this analysis ignores the contribution of the lattice ions Ca^{2+}, CO_3^{2-} in solution.
270 Several experimental studies have shown that the zeta potential of calcite is independent of
271 pH if the concentration of calcium (expressed in this paper as pCa, where p represents the
272 negative logarithm) is kept constant (e.g. [12, 21, 70]; see Fig. 3a). Moreover, other studies
273 have demonstrated a relationship between zeta potential and pCa (e.g. [4, 12, 54, 78]; see Fig.
274 4), and a strong dependence between the zeta potential of calcite and the excess of Ca^{2+} ions
275 at the mineral surface has been observed [33]. These data show that the development of
276 charge on the calcite surface is more complex than the simple protonation and deprotonation
277 reactions that occur at the surface sites of metal oxides (e.g. [71]). Instead, the lattice ions
278 Ca^{2+} and CO_3^{2-} adsorb onto the mineral surfaces through surface complexation reactions such
279 as (e.g. [29, 71, 79, 85])

280 $>CO_3H^0 + Ca^{2+} \Leftrightarrow >CO_3Ca^+ + H^+$ (9)

281 and, in the presence of CO_2, reactions such as

282 $>CaOH^0 + CO_2 \Leftrightarrow >CaCO_3^- + H^+$ (10)

283 $>CaOH^0 + CO_2 \Leftrightarrow >CaHCO_3^0$ (11)

284 As discussed below, the concentration dependent adsorption of these lattice ions (and other
285 potential determining ions) is the primary control on the zeta potential of calcite.

3.2. Potential determining ions

Surface diffraction studies have revealed well-ordered water layers a few Å (= 1×10^{-10} m) above the calcium and carbonate ions on the mineral surface [19, 20, 24, 29, 45]. This is the hydrolysis plane of Stipp [71] and the 0-plane invoked in various surface complexation models (SCMs) of the calcite-water interface ([29, 85]; see also Fig. 1a). Protonation and deprotonation reactions occur in this plane, but it does not contain the lattice ions Ca^{2+} and CO_3^{2-} or other adsorbed ion complexes. These are confined to the 1- and 2-planes (or the a- and b-planes), which here we associate with the inner and outer Helmholtz planes respectively (Fig. 1a). Most SCMs include ordered water layers at the 0-plane, and the pH-dependent protonation and deprotonation reactions (6) – (8) that occur at the sites defining the 0-plane [29, 71, 85]. However, the SCM of Heberling et al. [29] predicted that the charge at the 0-plane is only weakly pH dependent. The dominant surface species are $>CaOH^0$ and $>CaCO_3^-$, causing the 0-plane to be negatively charged across the pH range 5.5-11. Thus, unlike the >MeOH groups on oxide mineral surfaces, the calcite surface species $>CaOH^-$ and $>CaCO_3^-$ do not determine the pH dependence of the zeta potential. Rather, the potential at the OHP and, hence, the zeta potential, is instead controlled by adsorption of the potential-determining lattice ions Ca^{2+} or CO_3^{2-} at the 1- or 2-planes. The available evidence suggests that most of the adsorbed lattice PDIs are located at the 2-plane [29, 85].

Dissolution of calcite in aqueous solution is described by the following reaction:

$$CaCO_3\,(s) \Leftrightarrow Ca^{2+}\,(aq) + CO_3^{2-}\,(aq) \qquad (12)$$

The equilibrium conditions are defined by the pH, the concentration of the ionic species and, in open system conditions, the partial pressure of CO_2 (pCO_2) in solution [66, 68]. Moreover, the concentration of lattice ion species available to adsorb onto the calcite surface is controlled by the reactions [18]:

$$CO_3^{2-}(aq) + H_2O(l) \Leftrightarrow HCO_3^-(aq) + OH^-(aq) \quad (13)$$

$$HCO_3^-(aq) + H_2O(l) \Leftrightarrow H_2CO_3(aq) + OH^-(aq) \quad (14)$$

$$H_2CO_3(aq) \Leftrightarrow H_2O(l) + CO_2(g) \quad (15)$$

$$Ca^{2+}(aq) + H_2O(l) \Leftrightarrow Ca(OH)^+(aq) + H^+(aq) \quad (16)$$

$$Ca^{2+}(aq) + HCO_3^-(aq) \Leftrightarrow CaHCO_3^+(aq) \quad (17)$$

It can be seen from (12) - (17) that pH (and pCO_2) determines the Ca^{2+} and CO_3^{2-} concentrations in the solution at equilibrium. Apparent trends between zeta potential and pH therefore reflect the fact that pH and pCa are directly related at fixed pCO_2 (e.g. [64]). We confirm this experimentally in a later section. Thus, H^+ is not the key PDI for the calcite surface; rather, it is the lattice ion Ca^{2+} [4, 12, 21, 33, 51, 54]. Moreover, the PZC and IEP are not closely related. In principle, the PZC could be defined in terms of pH, as pH controls the protonation and deprotonation reactions at the 0-plane, However, in practice, the PZC is not observed over the pH range 5.5-11 [29]. The IEP must be defined in terms of pCa, or in terms of the concentration of other PDIs for the calcite surface such as Mg^{2+} as discussed below.

4. Experimental measurements of zeta potential

Published measurements of zeta potential in calcite and natural carbonates in aqueous solution range from +29 mV to -39 mV (Fig. 2). As discussed below, the zeta potential depends on the electrolyte concentration and composition, the nature of the calcite, sample preparation, experimental conditions and measurement method. However, limited reporting of the nature of the samples and experimental method, especially sample history, preparation and cleaning, and experimental conditions (especially pH, pCa and pCO_2), makes it challenging to systematically compare experimental data (see Table 1 for a summary). In this

section, we review and discuss the data published to date, and summarize the key controls on zeta potential.

4.1. Electrolyte concentration and composition

4.1.1. Effect of pH

Many studies have reported more negative values of zeta potential with increasing pH (e.g. [12, 18, 54, 78, 80]). For example, Thompson and Pownall [78] reported a close-to-linear relationship between zeta potential and pH (square data in Fig. 2a) using packed synthetic calcite and NaCl solution of ionic strength 5×10^{-3} M (filled squares) and NaCl/$NaHCO_3$ of ionic strength 5×10^{-4} M (open squares). Similarly, Vdovic [80] obtained a linear relationship between zeta potential and pH using natural carbonate powder samples suspended in 10^{-3} M NaCl electrolyte (filled and open circles in Fig. 2b). However, there are numerous exceptions (e.g. [11, 42, 46-48, 63, 67, 81]). For example, Siffert and Fimbel [63] found that the zeta potential of synthetic calcite at equilibrium pH (9.1; Table 1a) could be either positive or negative, dependent on the dispersed mass. Away from the equilibrium pH, the zeta potential decreased with either increasing or decreasing pH (open and grey stars in Fig. 2a). Vdović and Bišćan [81] (open circles in Fig. 2a) and Vdovic [80] (solid circles in Fig. 2a) observed similar behaviour. The latter reported zeta potential values that changed polarity with both increasing and decreasing pH, thus apparently defining two IEPs. Mahani et al. [46] [47] reported an increasingly negative zeta potential with increasing pH (grey triangles, diamonds and squares in Fig. 2a-b), contrary to the trends reported above. However, as discussed in the previous section, SCMs for calcite suggest the electrical potential at the mineral surface is only weakly pH dependent, and experimental data have shown that the zeta potential is independent of pH if pCa is held constant (Fig. 3). These data confirm that zeta potential is

not directly controlled by pH, but rather by the concentration of lattice ions such as Ca^{2+} and other PDIs discussed below.

4.1.2. Effect of pCa and pCO_3

Many authors have concluded that the principal PDIs for calcite are the lattice ions Ca^{2+} and CO_3^{2-} (e.g. [7, 12, 21, 33, 48, 54, 62, 63, 67, 78, 80, 81]). Consequently, the effect of Ca^{2+} on the zeta potential has been the topic of several experimental studies (e.g. [4, 12, 33, 54, 78]; see Fig. 4). The consistent observation in these studies is that decreasing pCa yields more positive zeta potential, consistent with increased adsorption of Ca^{2+} onto the calcite surface (Fig. 1). However, significant differences in the magnitude and polarity of the zeta potential, in the gradient of zeta potential vs. pCa ($d\zeta/dpCa$), and in the IEP (expressed as pCa), have been reported (Fig. 4; Table 1b). The zeta potential varies between +20mV and -26mV, depending on calcite type and experimental conditions. Most studies report a linear or close-to-linear relationship between zeta potential and pCa, especially for pCa values close to the IEP, with the gradient $d\zeta/dpCa$ in the range -8 to -15 mV/decade (Fig. 4). A linear relationship is consistent with Nernstian behaviour of the calcite surface and suggests the electrical double layer can be reasonably described by the simple Gouy–Chapman–Grahame model close to the IEP (e.g. [34]). This model is valid only when ions other than the lattice ions show no specific adsorption at the surface. The relationship between zeta potential and pCa can then be expressed as [21]:

$$\left.\frac{d\zeta}{dpCa}\right|_{\zeta\to 0} = \frac{-2.303\frac{kT}{ze}}{\left(1+\frac{C_d}{C_s}\right)\exp(\kappa\Delta)} \quad (18),$$

where k is Boltzmann's constant, T is the temperature, z is the valence of the PDI, e is the charge on an electron, κ is the Debye-Huckel reciprocal length, C_d and C_s are the capacitance

per unit area of the diffuse and Stern layers respectively, κ is the Debye-Huckel reciprocal length, and Δ is the distance of the shear plane from the Stern plane (see Fig. 1).

Zeta potential data obained at low ionic strength using the EPM method show a broadly consistent value of $d\zeta/dpCa$ of approximately -13 mV/decade (Fig. 4a). Equation (18) can be used to match these data using one value of $C_s \sim 0.4$ Fm^{-2} and Δ = zero. For comparison, Heberling et al. [29] fitted their zeta potential data using a more sophisticated SCM with C_s = 0.45 Fm^{-2} and Δ = 0.33 nm. Previous SCMs for calcite used unrealistically high C_s values of 10 – 100 Fm^{-2} [57, 79]. However, a number of recent studies have reported non-linear relationships between zeta potential and pCa (e.g. [11, 42, 88]; see Fig 4b). Moreover, a wide range of IEP (expressed as pCa) values have been reported (pCa of 1.92 – 4.5; Table 1b). As discussed in the following sections, the variability of these results might be attributed to differences in experimental conditions, including pCO_2, calcite type, measurement technique and the establishment of equilibrium. The effect of the carbonate ion on the zeta potential has received less attention than the calcium ion. The very limited data suggest that addition of CO_3^{2-} makes the zeta potential more negative, consistent with increased adsorption of CO_3^{2-} onto the calcite surface (e.g. [16, 51, 64]).

4.1.3. Effect of pMg and pSO_4

The magnesium ion is also compatible with the calcite crystal structure [8]. It has a direct influence on geochemical processes involving natural carbonates of mixed mineralogy such as dolomite [50] and is also abundant in natural brines, yet has received much less attention than Ca^{2+}. De Groot and Duyvis [14] suggested that Ca^{2+} and Mg^{2+} influence the zeta potential of calcite to a similar extent, but their dataset was very sparse, comprising just five measurements (two for Mg^{2+} and three for Ca^{2+}) at high pMg (i.e. at very low concentration; compare filled and open triangles in Fig. 5a). Smallwood [64] obtained a similar response

(compare filled and open squares in Fig. 5a) over the same concentration range. More recent studies have found that the zeta potential becomes more positive with decreasing pMg ([4, 11, 87]; see data represented by crosses, circles and diamonds in Fig. 5a). Alroudhan et al. [4] found that Mg^{2+} behaved identically to Ca^{2+} within experimental error over a wide range of pCa and pMg (0.4 – 3; compare filled and open diamonds). Moreover, they were the first to report an IEP in terms of pMg, which was identical to pCa_{IEP} within experimental error. However, data showing the effect of pMg on zeta potential are still very scarce, especially at low pMg.

A number of studies have also shown that the zeta potential is affected by the concentration of SO_4^{2-}, observing that the zeta potential becomes more negative with decreasing pSO_4 ([4, 64, 88]; Fig, 5b). Smallwood [64] argued that SO_4^{2-} is adsorbed onto the calcite mineral surface, similar to the lattice ions Ca^{2+}, Mg^{2+} and CO_3^{2-}, as indicated by its ability to reverse the polarity of the zeta potential (Fig. 5b). However, no other papers have reported an IEP in terms of pSO_4. Zhang and Austad [88] and Alroudhan et al. [4] both observed a linear relationship between zeta potential and pSO_4 for chalk and natural carbonate respectively, but the IEP was not encountered over the concentration range investigated (Fig. 5b). Data showing the effect of pSO_4 on zeta potential are still scarce and do not conclusively show that SO_4^{2-} is a PDI for the calcite surface.

4.1.4. Indifferent ions and total ionic strength

Ions other than Ca^{2+}, Mg^{2+}, CO_3^{2-} and SO_4^{2-} are generally assumed to be indifferent to the calcite mineral surface; they have little or no tendency to adsorb onto the surface. It is well known that the zeta potential decreases in magnitude with increasing concentration of indifferent ions such as Na^+, K^+, Cl^-, reflecting contraction of the electrical double layer (EDL; e.g. [36, 83]). Pierre et al. [54] obtained the same IEP (expressed as pH) on natural

426 calcite irrespective of the concentration of NaCl (0, 10^{-3}, 10^{-2} M), indicating that Na and Cl
427 are indifferent ions. Alroudhan et al. [4] found that the sensitivity of zeta potential to pCa (i.e.
428 dζ/dpCa) decreased as NaCl concentration increased, consistent with contraction of the EDL
429 reducing the absolute magnitude of the zeta potential (Fig. 4b and Table 1b). However, they
430 also found that the IEP (as pCa) decreased with increasing NaCl concentration, which is not
431 expected for indifferent ions. They suggested that at the high NaCl concentrations
432 investigated (up to 2M), the ability of Ca^{2+} ions to interact with calcite surface was reduced
433 due to contraction of the EDL and increasing occupancy of hydrated Na^{+} ions in the diffuse
434 layer. However, data to support this hypothesis are scarce; few studies have obtained zeta
435 potential measurements on calcite at high ionic strength (>0.1M).

436 **4.2. Partial pressure of CO_2**

437 Variations in pCO_2 across different experiments may be one factor that explains the variation
438 in reported values of IEP. In closed system experiments with controlled pCO_2, the very
439 limited data available suggest that the IEP (expressed as pH) decreases with increasing pCO_2
440 [29, 51]. Moreover, in open system experiments, Somasundaran and Agar [67] postulated
441 that pH_{IEP} was a function of mixing time of the sample powder in solution, due to an increase
442 in CO_2 concentration in the suspension. They used this mechanism to explain the decrease in
443 pH_{IEP} they observed with increased mixing time. The reported pH_{IEP} in closed system
444 experiments is generally higher than the value in open system experiments, consistent with
445 reduced access to CO_2 (Table 1a). The absence of, or limited access to, CO_2 in closed system
446 experiments causes a decrease in carbonic acid formation (equation 16) and in turn increases
447 pH_{IEP} [66].

448 The effect of pCO_2 on the IEP expressed as pCa or pMg is less well understood. No studies
449 have varied pCO_2 and pCa or pMg, or measured pCa or pMg whilst varying pCO_2 and pH.

Studies investigating the effect of pCa on zeta potential have typically been conducted in simple open or closed system conditions. In open system experiments, measured pCa_{IEP} lies in the range of 4.25 – 4.5 ([21, 33, 67]; Table 1b). In closed system experiments, reported pCa_{IEP} values have a wider range of 0.4 - 4 and are always lower than the pCa_{IEP} values reported in open system experiments (Table 1b). The broad range of pCa_{IEP} observed in closed system experiments might be attributed to different amounts of CO_2 dissolved into solution during preparation (e.g. [78]) or the type of calcite used (synthetic vs. natural; [54]; see also the next section). Recent studies of zeta potential on natural carbonates in closed system experiments consistently show the lowest values of pCa_{IEP} in the range 0.4-0.75 [4, 11, 42]. In closed system experiments, pCO_2 is fixed and, as we show later, lower pCa corresponds to lower pH. Lower pH is equivalent to higher pCO_2 (e.g. [29]; see also reactions 14–18).

4.3. Natural versus synthetic calcite

The zeta potential has been measured on a wide variety of calcite samples with differing nature and origin which can be broadly subdivided into three types: (1) synthetic calcite (pure precipitated crystalline calcium carbonate), (2) Iceland spar (pure crystalline calcite of natural origin) and (3) natural carbonate (composed mostly of calcite with inorganic material or organic matter). Data for Iceland spar and synthetic calcite show both positive and negative values for a given value of pH (Fig. 2; Table 1a) and pCa (Fig. 4a, Table 1b). The broad range of zeta potential values observed for a given pH may reflect differences in the concentrations of PDIs such as Ca^{2+} and Mg^{2+} that were not measured in the experiments; they may also reflect differences in pCO_2 or, as discussed below, the equilibration method. The range of values observed for a given pCa is more difficult to explain, but most likely

reflects differences in pCO_2 or the equilibration method; it may also reflect differences in the concentrations of other PDIs such as Mg^{2+} and SO_4^{2-}.

Data for natural calcite and carbonate rocks show less variability, with most studies returning negative values of zeta potential irrespective of pH; the few positive values in Fig. 2 were mostly obtained using natural brines rich in Ca^{2+} where, as we show later, positive zeta potential is expected. Berlin and Khabakov [7] reported negative zeta potentials on 115 natural carbonate samples irrespective of pH. Likewise, with relatively few exceptions, the zeta potential on natural samples has been found to be negative at high pCa and positive at low pCa, although there is some variability in pCa_{IEP} as discussed above (Fig. 4b). It has been suggested that the more negative zeta potentials typically observed in natural carbonates are due to the presence of organic matter incorporated in their structure during formation [80, 81]. For example, Vdovic [80] obtained negative zeta potential on two natural carbonate samples over the whole pH range (filled and open circles in Fig. 2b); however, they obtained a positive zeta potential on synthetic calcite (filled circles in Fig. 2a). Likewise, Cicerone et al. [12] found that natural (biogenetic) calcite (open triangles in Fig. 2b) bore a more negative zeta potential than pure calcite (filled triangles in Fig. 2a). However, the role of organic material in controlling the zeta potential of natural carbonates remains poorly understood.

4.4. Measurement technique

Measurements of zeta potential generally use either the electrophoretic mobility (EPM) method or the streaming potential method (SPM) introduced earlier. There appears to be no systematic difference in the reported IEP and both techniques have yielded a linear Nernstian relationship between zeta potential and pCa (Table 1; Fig. 4). However, only Alroudhan et al. [4] have compared the two techniques on the same (natural) calcite samples and electrolytes. Using the EPM method and natural (powdered) carbonate suspended in 0.05M NaCl

electrolyte, they obtained a linear regression between zeta potential and pCa with a gradient of -10.45mV/decade, which they fitted using equation (18) and values of C_s = 1.13 Fm^{-2} and $\Delta = 0$. Note that this gradient is lower than obtained in previous studies on similar samples (as discussed above; see also Fig. 4a) and the value of C_s used to obtain a match is higher. However, Alroudhan et al. [4] investigated electrolytes of higher total ionic strength than previous studies and their results suggest that C_s increases with increasing total ionic strength.

Using the SPM method and the same natural (intact) carbonates and electrolytes, Alroudhan et al. [4] obtained the same IEP (expressed as pCa) within experimental error, but the gradient of a linear regression through the data was approximately two times smaller at -5.10 mV/decade. They argued that the shear plane is further away from the mineral surface in intact natural samples as opposed to powdered samples owing to the complex topology of the pore-space (see also Vernhet et al. [82] for similar comparisons on other materials), and fitted the SPM data using equation (18) with the same value of C_s but a higher value of $\Delta = 0.245$nm. Thus differences in the observed sensitivity of zeta potential to pCa (or the concentration of other PDIs) may reflect differences in the measurement technique and/or the nature of the sample (intact versus powdered).

4.5. Establishment of equilibrium between sample and electrolyte

Most studies equilibrate the calcite-electrolyte systems of interest for 48 hours or less prior to measuring the zeta potential (Table 1). Only a few studies have investigated longer equilibration times (e.g. [4, 12, 29, 33, 67]). Some studies have reported equilibration times of an hour or less (e.g. [11, 18, 48, 58, 60]). Heberling et al. [29] investigated the difference between equilibrium and non-equilibrium measurements. In a study using natural intact limestone, Alroudhan et al. [4] found that the equilibrium pH in open system conditions was reached after 100 hours and sometimes more, and that it could take a factor of 2-3 times

longer to reach the equilibrium pCa (e.g. Fig. 6). Thus there is the risk that short equilibration times may not yield a stable equilibrium in pH and/or pCa, which will affect the measured zeta potential. Moreover, the equilibrium pH may be achieved before the equilibrium pCa, so assessing equilibration based on pH measurements alone may not be sufficient. As discussed above, values of the zeta potential on calcite are primarily controlled by pCa and the concentration of other PDIs such as Mg^{2+}, rather than pH. Therefore, it is important to ensure that equilibrium in the concentration of these PDIs has been reached prior to taking measurements. Inconsistent values of zeta potential obtained in some studies may reflect a lack of equilibration.

4.6. Summary of published zeta potential data on calcite

Published measurements to date have typically observed linear, Nernstian relationships between zeta potential and pH, and between zeta potential and pCa, especially for values of pH and pCa close to the IEP. However, despite the clear relationship between zeta potential and pH obtained in such studies, the proton is not a PDI for calcite, as varying pH whilst holding pCa constant yields constant zeta potential within experimental error. Moreover, surface complexation models suggest that the calcite surface remains negatively charged over the pH range 5.5-11, and the surface charge is only weakly dependent on pH. The zeta potential is controlled instead by the concentration-dependent adsorption of lattice ions Ca^{2+} and CO_3^{2-} in the Stern layer, and also by the adsorption of Mg^{2+} ions, although experimental data testing the effect of pMg are scarce. The few data available suggests that Mg^{2+} behaves identically to Ca^{2+} within experimental error. The SO_4^{2-} ion has also been suggested as a PDI for the calcite surface, but the evidence is not conclusive.

A wide range of values of IEP (expressed as pCa) have been observed, depending upon whether the sample is natural or artificial, whether the experiments are open or closed to

atmospheric CO_2, and the approach taken to equilibrate the sample and electrolyte prior to obtaining data. In open system experiments, measured pCa_{IEP} lies in the range of 4.25 – 4.5, but in closed system experiments, pCa_{IEP} has a wider range of 0.4 - 4 and is always lower than values reported in open system experiments. Natural samples generally show more negative values of zeta potential than artificial samples for a given value of pCa, and therefore yield lower values of pCa_{IEP}. Recent studies of zeta potential on natural carbonates in closed system experiments consistently show the lowest values of pCa_{IEP} in the range 0.4-0.75.

5. Measurements of zeta potential on natural limestone rock samples: Impact of rock type, PDI concentration and ionic strength

As outlined in the previous section, few studies have reported measurements of zeta potential in carbonates at conditions relevant to natural subsurface systems. Most have explored synthetic calcite and dilute electrolytes with much lower total ionic strength and PDI concentration than subsurface brines. Moreover, most did not employ an experimental method that established equilibrium conditions of pH, pCO_2 and PDI concentration relevant to subsurface carbonates. The aim of this section is to report new measurements of zeta potential relevant to natural systems, with a particular emphasis on determining (i) the relationship between pH and pPDI (Ca^{2+} and Mg^{2+}) in equilibrated calcite-electrolyte systems, given that no studies have measured pPDI whilst varying pH, or reported pH whilst varying pPDI, (ii) the effect of high concentrations of indifferent ions such as NaCl on the sensitivity of the zeta potential to pPDI, (iii) whether SO_4^{2-} is a PDI for the calcite mineral, and (iv) how the zeta potential is affected by pPDI over the concentration range found in natural brines. Only Alroudhan et al. [4] have probed this parameter space, and they used

only a single rock type. Here we investigate two further natural carbonates to determine whether the results are rock-type specific.

We used the SPM described by Jackson and co-workers [4, 35, 38, 39, 83] to measure the zeta potential. The SPM is applicable to intact natural samples, can be used to measure zeta potential at high ionic strength (> 2M), and can also be used during multiphase flow and at elevated temperature [1, 2, 4, 35, 37, 38, 83, 84]. The SPM measurements were complemented by chemical analysis of the effluent electrolyte, to monitor adsorption/desorption of ionic species during the experiments. The results have broad application to earth engineering processes such as hydrocarbon production and geological CO_2 storage, and we use them here to investigate the mechanisms that underpin the use of controlled injection brine compositions during waterflooding of hydrocarbon reservoirs [41, 74, 86, 87].

5.1. Materials and Experimental Method

We used two intact natural carbonate core samples that in x-ray diffraction (XRD) analysis appear to be identical pure limestone that differ only in age and permeability (Table 2). Also shown in Table 2 are the properties of the Portland Limestone samples investigated by Alroudhan et al. [4], which we compare to the new results presented here when possible. Samples were cleaned using the enhanced method reported in Alroudhan et al. [4]. The brines used were synthetic solutions of reagent-grade NaCl, $CaCl_2.2H_2O$, Na_2SO_4 and $MgCl_2.6H_2O$ salts (Sigma Aldrich, UK) in deionized water (DIW) from a filtered system with electrical conductivity below 1 μS/cm.

The equilibrium condition of carbonate/electrolyte/CO_2 discussed previously (see Fig. 6) was replicated following the approach of Alroudhan et al. [4]. NaCl electrolytes of varying concentrations (0.05 – 5M) were equilibrated by leaving offcuts of the tested carbonate

samples in a closed beaker containing an air gap to allow CO_2 to dissolve into solution, replicating the open-system conditions of carbonate deposition [76]. The pH of the NaCl electrolyte (measured using a Five-Go Mettler-Toledo pH meter with their 3-in-1 pH electrode LE438, implementing where necessary the manufacturer's recommended calibration and correction procedures at high ionic strength) and Ca^{2+} concentration (measured using Inductively Coupled Plasma Atomic Emission Spectroscopy, ICP-AES) were monitored until both reached constant value within experimental error. The equilibrium pH was found to be 8.3±0.1 for both Ketton and Estaillades, in agreement with Alroudhan et al. [4], and the equilibrium pCa was found to be 2.8±0.1 and 3.1±0.1, respectively. The equilibrated NaCl solutions were termed NaCl-EQ and were then used directly in zeta potential measurements, or were modified by addition of Ca^{2+}, Mg^{2+} and/or SO_4^{2-}.

The apparatus used to measure zeta potential in our SPM is closed to the atmosphere, and the second stage of equilibration prior to measuring the zeta potential was to ensure equilibrium between the electrolyte of interest (NaCl-EQ with or without the addition of Ca^{2+}, Mg^{2+} or SO_4^{2-}) and the rock sample at the closed-system conditions pertaining to a rock-brine system at depth. The rock sample was pre-saturated with the selected electrolyte at open-system conditions and then confined in the core holder at closed-system conditions, and the electrolyte was pumped through the sample from the (closed) inlet reservoir to the (closed) outlet reservoir and back again. The repeated flow of the electrolyte through the sample at closed system conditions mimics migration of the electrolyte into the carbonate rock at depth. At regular intervals, the electrical conductivity and pH of the electrolyte in the reservoirs was measured, and equilibrium was assumed to have been reached when the conductivity and pH of the electrolyte in each reservoir differed by <5%.

Electrolyte samples were analysed before and after the SPM experiments for key ions (Na^+, Ca^{2+}, Mg^{2+} and SO_4^{2-}). We used ICP-AES for cations and Ion Chromatography (IC) for

anions with appropriate dilution where necessary. The ICP-EAS analysis was carried out in the Analytical Chemistry Laboratory at the Natural History Museum London; the IC analysis was carried out in the TOTAL Laboratory for Reservoir Physics at Imperial College London. Instrument error was determined by using certified solutions containing Na^+, Ca^{2+}, Mg^{2+} and SO_4^{2-} and the error calculated from the standard deviation of five repeat measurements of each solution.

5.2. Design of experiments

We conducted two sets of experiments. In the first, the sensitivity of zeta potential to variations in NaCl concentration was tested using the equilibrated NaCl-EQ solutions described above. In these experiments, the concentration of Ca^{2+}, Mg^{2+} and SO_4^{2-} was dictated by the equilibration process; no additional salts containing these ionic species were added to the NaCl-EQ solutions. In the second, the sensitivity of the zeta potential to variations in Ca^{2+}, Mg^{2+} and SO_4^{2-} concentration was tested by adding salts containing these ionic species over the range found in natural brines (0.007 – 0.42M for Ca^{2+} and Mg^{2+}; 0.002 – 0.096M for SO_4^{2-}) to NaCl-EQ solutions of two different ionic strengths (0.5M and 2M). The 0.5M NaCl concentration represents seawater and is similar to the 'ZP brine' of Zhang and Austad [88] and Zhang et al. [87], allowing direct comparison of results. The 2M NaCl concentration represents the saline brines found in many saline aquifers and hydrocarbon reservoirs (e.g. [59]). In the second set of experiments, we investigated for the first time the relationship between pCa (or pMg) and pH. Note that in the experiments reported here, precipitation of salts such as $CaSO_4$ and $MgCO_3$ in the pore-space was prevented because each ion of interest (Ca^{2+}, Mg^{2+} or SO_4^{2-}) was added to NaCl-EQ electrolyte containing only trace or zero concentration of cations or anions other than Na^+ and Cl^-.

5.3. Results

Streaming potentials were measured using the paired-stabilization method of Vinogradov et al. [83] and typical raw results are shown in Fig. 7b,c. The stabilized voltage was plotted against the stabilized pressure difference across the sample for four different flow rates and a linear regression through the data yielded the streaming potential coupling coefficient and, via equation (3), the zeta potential. The uncertainty in the streaming potential coupling coefficient arising from the range of linear regressions that can be forced through the stabilized voltage and pressure data was used to determine the associated experimental error in zeta potential reported in the following sections.

5.3.1. Impact of Na^+ concentration on zeta potential

We begin by reporting the effect of NaCl concentration on zeta potential. When possible, we compare results from the Ketton and Estaillades samples investigated here against the Portland sample studied by Alroudhan et al. [4]. Fig. 7a shows the zeta potential as a function of NaCl concentration (in M) on a log-log scale for all three natural carbonate samples. A linear regression can be fitted to the data from each rock type (with $R^2 > 0.97$) but the gradient of the regression differs between samples. The Estaillades sample (filled triangles) shows the highest gradient (-8.08 ± 0.52 mV/M) and the Portland sample (filled grey diamonds) the lowest gradient (-5.08 ± 0.47 mV/M) with the Ketton sample (filled squares) in between (-6.11 ± 0.49 mV/M).

At low NaCl concentration (<0.1M) the zeta potential is negative and identical (within experimental error) for all three samples. However, as NaCl concentration increases, the zeta potentials diverge with $|\zeta_{\text{Portland}}| > |\zeta_{\text{Ketton}}| > |\zeta_{\text{Estaillades}}|$. Moreover, the zeta potential of the Estaillades samples becomes positive at NaCl concentration >1.9M, whereas the other two samples yield negative zeta potential over the entire concentration range investigated. The

665 inset plots 7b and 7c show there is no ambiguity in the polarity of the zeta potential: for a
666 NaCl concentration of 1.8M the streaming potential, and hence zeta potential, of the
667 Estaillades sample is clearly negative (-0.56mV ± 0.33) and becomes positive (0.72mV ±
668 0.33) for a NaCl concentration of 2M. As discussed above, Na^+ and Cl^- are believed to be
669 indifferent ions to the calcite mineral surface and their presence is expected to affect the
670 magnitude, but not the polarity, of the zeta potential (e.g. [23, 34, 54]).

671 5.3.2. Impact of pCa^{2+}, pMg^{2+} and pSO_4^{2-} on zeta potential

672 We next investigate the impact of the concentration of the confirmed and suggested PDIs
673 Ca^{2+}, Mg^{2+} and SO_4^{2-} on the zeta potential. We plot concentration as pPDI and, in all cases,
674 the highest pPDI values reported correspond to the equilibrium concentrations in the NaCl-
675 EQ electrolytes. Fig. 8a shows the impact of pCa and pMg on the zeta potential of
676 Estaillades, and the impact of pCa on the zeta potential of Ketton, for two different NaCl
677 concentrations (0.5M and 2M) typical of subsurface brines; also shown for comparison are
678 the data from Portland obtained by Alroudhan et al. [4]. We find that the zeta potential
679 consistently becomes more positive with decreasing pCa or pMg. Moreover, the response to
680 pCa and pMg is identical within experimental error for the Estaillades carbonate, irrespective
681 of NaCl concentration. Alroudhan et al. [4] also found that pCa and pMg behaved identically
682 for the Portland carbonate, although they investigated a lower NaCl concentration of 0.05M
683 and their data are not shown here.

684 The response of the zeta potential to pCa or pMg is generally sample specific and depends on
685 the NaCl concentration. At the lower (0.5M) NaCl concentration investigated here, Ketton
686 and Portland exhibit identical behaviour over the entire pCa range investigated: a linear
687 regression provides an excellent fit to the data ($R^2 > 0.98$) with a gradient of -4.5±0.25
688 mV/decade and an pCa_{IEP} of 0.5±0.03. A linear regression with the same gradient also

provides an excellent fit to the Estaillades data at the lower NaCl concentration investigated; however, pCa_{IEP} is much higher at 1.7±0.03. Nernstian (linear) behaviour is therefore always observed at the lower NaCl concentration over the entire pCa and pMg range investigated, but the IEP is different for the Estaillades sample. Fitting the Gouy-Chapman-Grahame model (equation 18) to these data yields C_s = 1 Fm^{-2} and Δ = 0.245 nm, similar to the values obtained for Portland carbonate by Alroudhan et al. [4] and within the range used by Heberling et al. [29].

At the higher (2M) NaCl concentration investigated here, the Ketton carbonate continues to show linear, Nernstian behaviour close to the IEP with a gradient and IEP identical to that obtained using 0.5M NaCl within experimental error, but the behaviour becomes non-linear (non-Nernstian) away from the IEP at high pCa. The Portland sample shows linear, Nernstian behaviour over the entire pCa range investigated with an identical IEP within experimental error but a lower gradient of -2.86±0.25 mV/decade. The Estaillades carbonate exhibits notably different behaviour, with the zeta potential remaining positive over the entire pCa/pMg range investigated, and non-Nernstian behaviour at high pCa. Cicerone et al. [12] also observed non-Nernstian behavior far from IEP and related that to variations in the Stern layer capacitance or to breakdown of the Gouy-Chapman-Grahame model.

Increasing pSO_4 consistently yields more positive zeta potential, although the sensitivity is much less than that observed when varying pCa or pMg (Fig. 8b). A linear regression yields a good fit to the data at the lower NaCl concentration investigated here ($R^2 > 0.92$) with a consistent gradient of 0.84 ±0.2 mV/decade for both the Estaillades and Portland carbonates. A key feature is that an apparent IEP of pSO_4 = 1.59 ±0.2 is observed for the Estaillades sample in 2M NaCl electrolyte. It is also notable that the difference in absolute zeta potential between the different carbonate samples observed in Fig. 7 persists in Fig. 8, with $|\zeta_{Portland}| > |\zeta_{Ketton}| > |\zeta_{Estaillades}|$.

714 5.3.3. Relationship between pH and pCa or pMg

715 Fig. 9a shows the relationship between the equilibrium pH and pCa or pMg obtained across
716 all of the experiments reported here. A linear regression provides an excellent fit to the data
717 ($R^2 > 0.98$) with a gradient of 0.81, irrespective of NaCl concentration, rock sample or PDI
718 varied, although the value of pH is consistently higher in the experiments varying pMg as
719 compared to those varying pCa. These experimental data confirm that equilibrium pH and
720 pPDI are related at fixed pCO_2 via equations (14) – (18). It is possible to plot the data
721 obtained here against pH and obtain an apparently strong correlation (Fig. 9b) even though
722 pCa and pMg were the controlled parameters. The relation between pH and pCa or pMg
723 obtained here is consistent with model predictions (e.g. PHREEQC; [55]). However, it has
724 not previously been demonstrated in properly equilibrated experiments where zeta potential
725 was also measured, or over such a wide range of pCa.

726 **5.4. Discussion**

727 5.4.1. Impact of indifferent ions

728 The results presented here show a clear relationship between the concentration of indifferent
729 ions Na^+ and Cl^- and the zeta potential on natural carbonate (Fig. 7). Such a relationship is
730 expected owing to collapse of the double layer with increasing ionic strength, but if double
731 layer collapse is the only control on zeta potential, then the zeta potential should be
732 proportional to the logarithm of NaCl concentration (as a proxy for ionic strength; e.g. [27]).
733 Consequently, the dependence of zeta potential on NaCl concentration observed in Fig. 7
734 cannot result only from double layer collapse. Fig. 10 shows the equilibrium pCa and pSO_4 as
735 a function of NaCl concentration, corresponding to the zeta potential data shown in Fig. 7.
736 Note that pMg remained large and approximately constant at 4.19±0.03 for all samples

737 irrespective of NaCl concentration (i.e. the Mg^{2+} concentration is small). pCa generally
738 decreases with increasing NaCl concentration (Fig. 10a); hence, given that zeta potential
739 becomes more positive with decreasing pCa, these data are consistent with the more positive
740 zeta potential observed with increasing NaCl concentration in Fig. 7. However, the sensitivity
741 decreases at high NaCl concentration, moreover, these data do not explain the polarity change
742 of the zeta potential observed for the Estaillades carbonate. This remains a curious feature of
743 the new data obtained here and may suggest that Na^+ is not in fact an indifferent ion to the
744 calcite surface in some circumstances, as suggested by [29, 44].

745 5.4.2. Impact of carbonate type

746 The results obtained here also show that natural carbonate samples that appear identical in
747 XRD display different zeta potential behaviour. The Estaillades carbonate, in particular,
748 behaves differently to the Ketton and Portland carbonates, showing inversion of the zeta
749 potential with increasing NaCl concentration (Fig. 7), higher values of pCa_{IEP}/pMg_{IEP}
750 compared to Ketton and Portland (Fig. 8a), and also an apparent IEP expressed as pSO_4 (Fig.
751 8b). The Estaillades carbonate released the least SO_4^{2-} during equilibration with the NaCl
752 solutions, while the Portland sample released the most SO_4^{2-} (Fig. 10b), consistent with the
753 observed differences in zeta potential ($\zeta_{Portland} > \zeta_{Ketton} > \zeta_{Estaillades}$) in Figs. 7 and 8. We
754 hypothesize that Ketton and Portland contain undetected sources of SO_4^{2-} which affects the
755 pristine zeta potential, yielding more negative values and lower pCa_{IEP} than Estaillades.
756 Natural carbonates can incorporate a number of different minerals, including clays, organic
757 matter, apatite, anhydrite or quartz, that yield a more negative zeta potential than pure calcite
758 [12, 65, 66]. Our data therefore suggest that the behaviour of the natural Ketton and Portland
759 carbonate samples investigated here is affected by the presence of impurities such as
760 anhydrite. In contrast, the behaviour of the Estaillades sample is consistent with the ionic

strength effect as calculated with a Pitzer model for a calcite-atmospheric CO_2 equilibrium solution [55].

The contrasting behaviour of Estaillades carbonate may also reflect differences in the affinity of Ca^{2+} and CO_3^{2-} for the mineral surface. Pierre et al. [54] suggested that the IEP is governed by the relative magnitude of the equilibrium constants K_{Ca} and K_{CO3} governing the adsorption of Ca^{2+} and CO_3^{2-} ions on the calcite mineral surface. The IEP shifts to lower pCa if $K_{CO3} > K_{Ca}$; that is, if the calcite surfaces show greater affinity for CO_3^{2-} than Ca^{2+}. Pierre et al. [54] found the IEP differed for synthetic and natural calcite and argued that this reflected the differing affinity for Ca and CO_3. The Pierre et al. model suggests that the Estaillades carbonate investigated here has a much lower affinity to CO_3^{2-} (and greater affinity to Ca^{2+}) than the Ketton and Portland carbonates at equilibrium conditions.

5.1.3. SO_4 as a PDI for calcite

Several studies have suggested that the SO_4^{2-} ion is a PDI for calcite (e.g. [64, 88]). However, these studies did not measure changes in pCa or pMg in response to changing pSO_4. Here, we find that SO_4^{2-} has only a minor influence on the zeta potential of natural carbonate (Fig. 8b). At low ionic strength (0.5M NaCl), the change in pSO_4 correlates to a change in pCa (Fig. 11a) which can explain the change in zeta potential (Fig. 11b). We observe a linear relationship between zeta potential and pCa with a similar gradient (5.1 mV/decade; R^2>0.85) to that obtained in the experiments where pCa was varied (4.5 mV/decade). However, at high ionic strength (2M NaCl), pCa is relatively insensitive to pSO_4 (Fig. 11a), yet the zeta potential still varies in response to changing pSO_4 and changes polarity from positive to negative. Moreover, there is not a clear correlation between pCa and zeta potential (Fig. 11b). It may be that small changes in pCa, pMg and even pNa within experimental error all contribute to the observed change in zeta potential, as it is only c. 1 mV in magnitude and

785 close to the IEP. Geochemical modelling beyond the scope of the paper is required to test this
786 hypothesis.

787

788 5.1.4. Implications for wettability alteration and hydrocarbon recovery in carbonate
789 reservoirs

790 In carbonate rock formations with positively charged mineral surfaces, an attractive
791 electrostatic force will act between the mineral surfaces and the negatively charged oil-brine
792 interface, promoting wettability alteration to oil-wet conditions (e.g. [10, 31]). Several studies
793 have suggested that carbonate rocks saturated with natural brines rich in Ca^{2+} and Mg^{2+} ions
794 have positively charged mineral surfaces so are likely to be oil-wet (e.g. [4, 11, 38, 46, 47]).
795 The wettability of a reservoir plays a key role in the efficiency with which the oil can be
796 produced. However, we find here considerable variability in the IEP expressed as pCa,
797 suggesting that some carbonates will be positively charged in contact with natural brines, and
798 others will not. The SPM used here is a suitable technique to determine the zeta potential of
799 intact reservoir rock samples saturated with natural brine (e.g. [38]).

800 In many reservoirs, water is injected to maintain the pressure and displace oil towards
801 production wells. If the concentration of Ca^{2+} or Mg^{2+} in the injected water can be modified
802 to fall below the IEP, either selectively or by bulk dilution in a process termed 'controlled
803 salinity waterflooding' (CSW), the zeta potential will change polarity from positive to
804 negative. The polarity change leads to electrostatic repulsion between the mineral surfaces
805 and the negatively charged oil-brine interface. This may promote wettability alteration to
806 water-wet conditions, releasing previously adsorbed oil from the calcite mineral surfaces and
807 therefore improving oil recovery (e.g. [47]).

Most previous reported values of the IEP expressed as pCa suggest that considerable reduction in Ca concentration is required to change the polarity of calcite (Table 1). However, our results suggest that far less dilution may be required in some natural carbonates (e.g. Ketton and Portland); in others, the IEP may never be encountered and the mineral surfaces may remain positively charged (e.g. Estaillades). The carbonate-rock-specific relationship between zeta potential and PDI concentration observed here may explain why CSW in some cases yields increased recovery and in other cases does not (e.g. [3, 59]). Future work relevant to CSW should focus on testing the link between brine composition, zeta potential and increased oil recovery using integrated experiments with consistent materials and experimental conditions (e.g. [37]).

6. Conclusions

Experimental studies of the zeta potential of calcite and carbonate have reported a broad range of values with numerous inconsistent results. Yet the primary data source to understand calcite surface charge comprises measurements of zeta potential, so it is important to understand the key controls on zeta potential and why studies have reported apparently contradictory values. A comprehensive review of the literature, supplemented by experimental data new to this study, suggests that:

1. The potential determining ions (PDIs) for the carbonate mineral surface are the lattice ions Ca^{2+}, Mg^{2+} and CO_3^{2-}. The zeta potential is controlled by the concentration-dependent adsorption of these ions within the Stern layer, primarily at the Outer Helmholtz Plane (OHP).
2. Given (1), the Iso-Electric Point (IEP) at which the zeta potential is zero should be expressed as pCa (or pMg). It should not be reported as pH, similar to most metal oxides.

3. The pH does not directly control the zeta potential. Varying the pH whilst holding pCa constant yields constant zeta potential. The pH affects the zeta potential only by moderating the equilibrium pCa for a given CO_2 partial pressure (pCO_2).
4. Experimental studies that appear to yield a systematic relationship between pH and zeta potential are most likely observing the relationship between pCa and zeta potential, with pCa responding to the change in pH. New experimental data presented here show a consistent linear relationship between equilibrium pH and equilibrium pCa or pMg irrespective of sample or solution ionic strength.
5. The surface charge is weakly dependent on pH through protonation and deprotonation reactions that occur within a hydrolysis layer immediately adjacent to the mineral surface. The Point of Zero Charge (PZC) at which the surface charge is zero could be expressed as pH, but surface complexation models suggest the surface is negatively charged over the pH range 5.5-11.
6. Several studies have suggested that SO_4^{2-} is also a PDI for the calcite surface, but new experimental data presented here indicate that the value of pSO_4 may affect zeta potential only by moderating the equilibrium pCa. Modelling will be required to provide a more thorough interpretation of the new data.
7. Natural carbonate typically yields a more negative zeta potential than synthetic calcite, most likely due to the presence of impurities including clays, organic matter, apatite, anhydrite or quartz, that yield a more negative zeta potential than pure calcite. New data presented here show that apparently identical natural carbonates display differing zeta potential behavior, most likely due to the presence of small volumes of these impurities.
8. It is important to ensure that equilibrium, defined in terms of the concentration of PDIs, has been reached prior to taking measurements. Inconsistent values of zeta potential obtained in some studies may reflect a lack of equilibration.

9. The data collated and reported here have broad application in engineering processes including the manufacture of paper and cement, the geologic storage of nuclear waste and CO_2, and the production of oil and gas.

Acknowledgments

TOTAL are thanked for partially funding Jackson under the TOTAL Chairs programme at Imperial College London, and for supporting Vinogradov through the TOTAL Laboratory for Reservoir Physics where the experiments reported were undertaken. Petroleum Development Oman are thanked for supporting Al Mahrouqi.

References

[1] Al Mahrouqi D, Vinogradov J, Jackson M. Understanding controlled salinity waterflooding in carbonates using streaming potential measurements. Proceedings of the SPE Latin American and Caribbean Petroleum Engineering Conference, 18-20 November, Quito, Ecuador SPE-177242-MS2015.

[2] Al Mahrouqi D, Vinogradov J, Jackson MD. Temperature dependence of the zeta potential in intact natural carbonates. Geophysical Research Letters. 2016.

[3] Alotaibi MB, Azmy R, Nasr-El-Din HA. Wettability challenges in carbonate reservoirs. Proceedings of the SPE Improved Oil Recovery Symposium, 24-28 April, Tulsa, Oklahoma, USA SPE-129972-MS2010.

[4] Alroudhan A, Vinogradov J, Jackson M. Zeta potential of intact natural limestone: Impact of potential-determining ions Ca, Mg and SO_4. Colloids and Surfaces A: Physicochemical and Engineering Aspects. 2016.

[5] Bapat JD. Mineral admixtures in cement and concrete: CRC Press, Taylor & Francis, New York 2012.

[6] Bard AJ, Faulkner LR, Leddy J, Zoski CG. Electrochemical methods: Fundamentals and applications: Wiley, New York; 1980.

[7] Berlin TS, Khabakov AV. Difference in the electrokinetic potentials of carbonate sedimentary rocks of different origin and composition. Geochemistry. 1961:217-30.

[8] Bragg WL. Atomic structure of minerals: Cornell University Press, New York; 1950.

[9] Buckley J, Liu Y, Monsterleet S. Mechanisms of wetting alteration by crude oils. SPE Journal. 1998;3:54-61.

[10] Buckley J, Takamura K, Morrow N. Influence of electrical surface charges on the wetting properties of crude oils. SPE Reservoir Engineering. 1989;4:332-40.

[11] Chen L, Zhang G, Wang L, Wu W, Ge J. Zeta potential of limestone in a large range of salinity. Colloids and Surfaces A: Physicochemical and Engineering Aspects. 2014;450:1-8.

[12] Cicerone DS, Regazzoni AE, Blesa MA. Electrokinetic properties of the calcite water interface in the presence of magnesium and organic-matter. Journal of Colloid and Interface Science. 1992;154:423-33.

[13] Davis JA, Kent D. Surface complexation modeling in aqueous geochemistry. Reviews in Mineralogy and Geochemistry. 1990;23:177-260.

[14] De Groot K, Duyvis E. Crystal form of precipitated calcium carbonate as influenced by adsorbed magnesium ions. Nature. 1966;212:183-4.

[15] Delgado AV, Gonzalez-Caballero F, Hunter RJ, Koopal LK, Lyklema J. Measurement and interpretation of electrokinetic phenomena. Journal of Colloid and Interface Science. 2007;309:194-224.

[16] Douglas H, Walker R. The electrokinetic behaviour of Iceland Spar against aqueous electrolyte solutions. Transactions of the Faraday Society. 1950;46:559-68.

[17] Dukhin SS, Deriaguine BV. Surface and colloid science: Electrokinetic phenomena: John Wiley & Sons, New York; 1974.

[18] Eriksson R, Merta J, Rosenholm JB. The calcite/water interface: Surface charge in indifferent electrolyte media and the influence of low-molecular-weight polyelectrolyte. Journal of Colloid and Interface Science. 2007;313:184-93.

[19] Fenter P, Geissbühler P, DiMasi E, Srajer G, Sorensen LB, Sturchio NC. Surface speciation of calcite observed in situ by high-resolution X-ray reflectivity. Geochimica et Cosmochimica Acta. 2000;64:1221-8.

[20] Fenter P, Sturchio NC. Mineral–water interfacial structures revealed by synchrotron X-ray scattering. Progress in Surface Science. 2004;77:171-258.

[21] Foxall T, Peterson GC, Rendall HM, Smith AL. Charge determination at calcium salt/aqueous solution interface. Journal of the Chemical Society, Faraday Transactions 1: Physical Chemistry in Condensed Phases. 1979;75:1034-9.

[22] Fuerstenau MC, Gutierrez G, Elgillani DA. The influence of sodium silicate in non metallic flotation systems. Transactions of the AIME. 1968;241:319.

[23] Garrels RM, Christ CL. Solutions, minerals, and equilibria: Harper & Row; 1965.

[24] Geissbühler P, Fenter P, DiMasi E, Srajer G, Sorensen L, Sturchio N. Three-dimensional structure of the calcite–water interface by surface X-ray scattering. Surface Science. 2004;573:191-203.

[25] Glover P. Comment on "Examination of a Theoretical Model of Streaming Potential Coupling Coefficient". International Journal of Geophysics. 2015;2015.

[26] Glover PW, Jackson MD. Borehole electrokinetics. The Leading Edge. 2010;29:724-8.

[27] Glover PWJ, Walker E, Jackson MD. Streaming-potential coefficient of reservoir rock: A theoretical model. Geophysics. 2012;77:D17-D43.

[28] Gomari KR, Hamouda A, Denoyel R. Influence of sulfate ions on the interaction between fatty acids and calcite surface. Colloids and Surfaces A: Physicochemical and Engineering Aspects. 2006;287:29-35.

[29] Heberling F, Trainor TP, Lützenkirchen J, Eng P, Denecke MA, Bosbach D. Structure and reactivity of the calcite–water interface. Journal of Colloid and Interface Science. 2011;354:843-57.

[30] Hester RE, Harrison RM. Carbon capture: Sequestration and storage: Royal Society of Chemistry, London; 2010.

[31] Hiorth A, Cathles LM, Madland MV. The impact of pore water chemistry on carbonate surface charge and oil wettability. Transport in Porous Media. 2010;85:1-21.

[32] Hohl H, Sigg L, Stumm W. Characterization of surface chemical properties of oxides in natural waters: The role of specific adsorption in determining the surface charge. In: K. MC, L. JO, (editors). Particulates in Water. Vol. 189: Advances in Chemistry; American Chemical Society: Washington, DC; 1980. Chapter 1. p. 1-31.

[33] Huang YC, Fowkes FM, Lloyd TB, Sanders ND. Adsorption of calcium ions from calcium chloride solutions onto calcium carbonate particles. Langmuir. 1991;7:1742-8.

[34] Hunter RJ. Zeta potential in colloid science : Principles and applications: Academic Press, New Yotk; 1981.

[35] Jaafar MZ, Vinogradov J, Jackson MD. Measurement of streaming potential coupling coefficient in sandstones saturated with high salinity NaCl brine. Geophysical Research Letters. 2009;36.

[36] Jackson MD. Self-potential: Tools and techniques, in Treatise on Geophysics, vol. 11, 2nd ed., edited by G. Schubert, chap. 9, Elsevier,Oxford. 2015.

[37] Jackson MD, Al-Mahrouqi D, Vinogradov J. Zeta potential in oil-water-carbonate systems and its impact on oil recovery during controlled salinity water-flooding. Scientific Reports. 2016;6:37363.

[38] Jackson MD, Vinogradov J. Impact of wettability on laboratory measurements of streaming potential in carbonates. Colloids and Surfaces A-Physicochemical and Engineering Aspects. 2012;393:86-95.

[39] Jackson MD, Vinogradov J, Saunders JH, Jaafar MZ. Laboratory measurements and numerical modeling of streaming potential for downhole monitoring in intelligent wells. SPE Journal. 2011;16:625-36.

[40] Jouniaux L, Pozzi JP. Streaming potential and permeability of saturated sandstones under triaxial stress: Consequences for electrotelluric anomalies prior to earthquakes. Journal of Geophysical Research: Solid Earth. 1995;100:10197-209.

[41] Karoussi O, Hamouda AA. Imbibition of sulfate and magnesium ions into carbonate rocks at elevated temperatures and their influence on wettability alteration and recovery. Energy & Fuels. 2007;21:2138-46.

[42] Kasha A, Al-Hashim H, Abdallah W, Taherian R, Sauerer B. Effect of Ca^{2+}, Mg^{2+} and SO_4^{2-} ions on the zeta potential of calcite and dolomite particles aged with stearic acid. Colloids and Surfaces A: Physicochemical and Engineering Aspects. 2015;482:290-9.

[43] Kruyt H, Overbeek J. An introduction to physical chemistry for biologists and medical students: Holt, Rinehart and Winston, New York; 1960.

[44] Lee SS, Heberling F, Sturchio NC, Eng PJ, Fenter P. Surface charge of the calcite (104) terrace Mmeasured by Rb^+ adsorption in aqueous solutions using resonant anomalous X-ray reflectivity. The Journal of Physical Chemistry C. 2016;120:15216-23.

[45] Magdans U, Torrelles X, Angermund K, Gies H, Rius J. Crystalline order of a water/glycine film coadsorbed on the (104) calcite surface. Langmuir. 2007;23:4999-5004.

[46] Mahani H, Keya AL, Berg S, Bartels W-B, Nasralla R, Rossen WR. Insights into the mechanism of wettability alteration by low-salinity flooding (LSF) in carbonates. Energy & Fuels. 2015;29:1352-67.

[47] Mahani H, Keya AL, Berg S, Nasralla R. Electrokinetics of carbonate/brine interface in low-salinity waterflooding: Effect of brine salinity, composition, rock type, and pH on ζ-potential and a surface-complexation model. SPE Journal. 2016.

[48] Mishra S. The electrokinetics of apatite and calcite in inorganic electrolyte environment. International Journal of Mineral Processing. 1978;05:69-83.

[49] Morgan F, Williams E, Madden T. Streaming potential properties of westerly granite with applications. Journal of Geophysical Research: Solid Earth. 1989;94:12449-61.

[50] Morse JW. The surface chemistry of calcium carbonate minerals in natural waters: An overview. Marine Chemistry. 1986;20:91-112.

[51] Moulin P, Roques H. Zeta potential measurement of calcium carbonate. Journal of Colloid and Interface Science. 2003;261:115-26.

[52] Overbeek JTG. Electrochemistry of the double layer. In: Kruyt HR, (editor). Colloid Science. Vol. 1: Elsevier, Amsterdam-Huston-New York-London; 1952. p. 115-93.

[53] Patil M, Shivakumar K, Prakash S, Rao RB. Effect of organic reagents on the zeta potentials of graphite, quartz and calcite minerals. Journal of Surface Science and Technology. 1998;14:280-5.

[54] Pierre A, Lamarche J, Mercier R, Foissy A, Persello J. Calcium as potential determining ion in aqueous calcite suspensions. Journal of Dispersion Science and Technology. 1990;11:611-35.

[55] Plummer LN, Busenberg E. The solubilities of calcite, aragonite and vaterite in CO_2-H_2O solutions between 0 and 90°C, and an evaluation of the aqueous model for the system $CaCO_3$-CO_2-H_2O. Geochimica et Cosmochimica Acta. 1982;46:1011-40.

[56] Pokrovsky O, Mielczarski J, Barres O, Schott J. Surface speciation models of calcite and dolomite/aqueous solution interfaces and their spectroscopic evaluation. Langmuir. 2000;16:2677-88.

[57] Pokrovsky O, Schott J. Surface chemistry and dissolution kinetics of divalent metal carbonates. Environmental Science & Technology. 2002;36:426-32.

[58] Rao KH, Antti B-M, Forssberg E. Mechanism of oleate interaction on salt-type minerals part I. Adsorption and electrokinetic studies of calcite in the presence of sodium oleate and sodium metasilicate. Colloids and Surfaces. 1989;34:227-39.

[59] Romanuka J, Hofman J, Ligthelm DJ, Suijkerbuijk BMJM, Marcelis AHM, Oedai S, et al. Low salinity EOR in carbonate Proceedings of the SPE Improved Oil Recovery Symposium, 14-18 April, Tulsa, Oklahoma, USA SPE-153869-MS2012.

[60] Sampat Kumar VY, Mohan N, Biswas AK. Fundamental studies on the role of carbon dioxide in a calcite flotation system. Transactions of the AIME. 1971;250:182-6.

[61] Schindler PW, Stumm W. The surface chemistry of oxides, hydroxides, and oxide minerals. In: Stumm W, (editor). Aquatic Surface Chemistry: Chemical Processes at the Particle-Water Interface: John Wiley & Sons, New York; 1987. p. 83-110.

[62] Schramm LL, Mannhardt K, Novosad JJ. Electrokinetic properties of reservoir rock particles. Colloids and Surfaces. 1991;55:309-31.

[63] Siffert D, Fimbel P. Parameters affecting the sign and magnitude of the eletrokinetic potential of calcite. Colloids and Surfaces. 1984;11:377-89.

[64] Smallwood P. Some aspects of the surface chemistry of calcite and aragonite Part I: An electrokinetic study. Colloid and Polymer Science. 1977;255:881-6.

[65] Smani M, Blazy P, Cases J. Beneficiation of sedimentary Moroccan phosphate ores. Transactions of the AIME. 1975;258:168-82.

[66] Somasundaran P. Encyclopedia of surface and colloid science: CRC press Taylor & Francis, New York; 2006.

[67] Somasundaran P, Agar G. The zero point of charge of calcite. Journal of Colloid and Interface Science. 1967;24:433-40.

[68] Somasundaran P, Amankonah JO, Ananthapadmabhan K. Mineral-solution equilibria in sparingly soluble mineral systems. Colloids and Surfaces. 1985;15:309-33.

[69] Somasundaran P, Deo, Namita D, Puspendu Natarajan KA. Role of biopolymers on bacterial adhesion and mineral beneficiation. Minerals and Metallurgical Processing. 2005;22:1-11.

[70] Sondi I, Bišćan J, Vdović N, Škapin SD. The electrokinetic properties of carbonates in aqueous media revisited. Colloids and Surfaces A: Physicochemical and Engineering Aspects. 2009;342:84-91.

[71] Stipp S. Toward a conceptual model of the calcite surface: Hydration, hydrolysis, and surface potential. Geochimica et Cosmochimica Acta. 1999;63:3121-31.

[72] Stipp S, Eggleston C, Nielsen B. Calcite surface structure observed at microtopographic and molecular scales with atomic force microscopy (AFM). Geochimica et Cosmochimica Acta. 1994;58:3023-33.

[73] Stipp SL, Hochella MF. Structure and bonding environments at the calcite surface as observed with X-ray photoelectron spectroscopy (XPS) and low energy electron diffraction (LEED). Geochimica et Cosmochimica Acta. 1991;55:1723-36.

[74] Strand S, Hognesen EJ, Austad T. Wettability alteration of carbonates - Effects of potential determining ions (Ca^{2+} and SO_4^{2-}) and temperature. Colloids and Surfaces A: Physicochemical and Engineering Aspects. 2006;275:1-10.

[75] Stumm W. Chemistry of the solid-water interface: Processes at the mineral-water and particle-water interface in natural systems: John Wiley & Sons, New Yotk; 1992.

[76] Stumm W, Morgan JJ. Aquatic chemistry: chemical equilibria and rates in natural waters: John Wiley & Sons, New York; 2012.

[77] Stumm W, Wehrli B, Wieland E. Surface complexation and its impact on geochemical kinetics. Croat Chem Acta. 1987;60:429.

[78] Thompson DW, Pownall PG. Surface electrical-properties of calcite. Journal of Colloid and Interface Science. 1989;131:74-82.

[79] Van Cappellen P, Charlet L, Stumm W, Wersin P. A surface complexation model of the carbonate mineral-aqueous solution interface. Geochimica et Cosmochimica Acta. 1993;57:3505-18.

[80] Vdovic N. Electrokinetic behaviour of calcite - The relationship with other calcite properties. Chemical Geology. 2001;177:241-8.

[81] Vdović N, Bišćan J. Electrokinetics of natural and synthetic calcite suspensions. Colloids and Surfaces A: Physicochemical and Engineering Aspects. 1998;137:7-14.

[82] Vernhet A, Bellon-Fontaine M, Doren A. Comparison of three electrokinetic methods to determine the zeta potential of solid surfaces. Journal de Chimie Physique. 1994;91:1728-47.

[83] Vinogradov J, Jaafar MZ, Jackson MD. Measurement of streaming potential coupling coefficient in sandstones saturated with natural and artificial brines at high salinity. Journal of Geophysical Research-Solid Earth. 2010;115:B12204.

[84] Vinogradov J, Jackson MD. Multiphase streaming potential in sandstones saturated with gas/brine and oil/brine during drainage and imbibition. Geophysical Research Letters. 2011;38:L01301.

[85] Wolthers M, Charlet L, Van Cappellen P. The surface chemistry of divalent metal carbonate minerals; a critical assessment of surface charge and potential data using the charge distribution multi-site ion complexation model. American Journal of Science. 2008;308:905-41.

[86] Yousef AA, Al-Saleh SH, Al-Kaabi A, Al-Jawfi MS. Laboratory investigation of the impact of injection-water salinity and ionic content on oil recovery from carbonate reservoirs. SPE Reservoir Evaluation & Engineering. 2011;14:578-93.

[87] Zhang P, Tweheyo MT, Austad T. Wettability alteration and improved oil recovery by spontaneous imbibition of seawater into chalk: Impact of the potential determining ions Ca^{2+}, Mg^{2+}, and SO_4^{2-}. Colloids and Surfaces A: Physicochemical and Engineering Aspects. 2007;301:199-208.

[88] Zhang PM, Austad T. Wettability and oil recovery from carbonates: Effects of temperature and potential determining ions. Colloids and Surfaces A: Physicochemical and Engineering Aspects. 2006;279:179-87.

Tables

Table 1: Summary of published zeta potential of calcite and carbonate. Table 1a reports studies focusing on the effect of varying pH. Table 1b reports studies focusing on the effect of varying pCa.

Table 1a.

Material	Method	Background electrolyte	Equilibrium condition	Equilibration time (hr)	Equilibrium pH (pH_{EQ})	Open vs. closed system	Zeta potential at EQ.	pH_{IEP}	IEP determination	Reference
Iceland spar	SPM	Deionized water (HNO_3/NaOH)	Calcite/water /air	1440	8.2	Open	Positive	8.2	Extrapolated	[67]
Iceland spar	SPM	SiO_2/Na_2O	Calcite/water	N/A	9.8	Closed	Positive	10.8	Direct	[22]
Iceland spar	SPM	Deionized water	Calcite/water /CO_2	N/A	6.55	$pCO_2 = 0.23$	Negative	6.55	Direct	[51]
					7.05	$pCO_2 = 0.023$	Negative	7.05		
Iceland spar	SPM	Deionized water	Calcite/water /CO_2	24 - 720	5.8	$pCO_2 = 1$	Negative	6.5	Direct	[29]
					7.5	$pCO_2 = 10^{-3.44}$	Negative	8.8		
					8.3	$pCO_2 = 10^{-5.2}$	Negative	9.4		
Iceland spar	EPM	Deionized water	Calcite/water	24	N/A	Closed	Negative	5.4	Extrapolated	[42]
Iceland spar	EPM	Deionized water	Calcite/water /CO_2	1-2	N/A	Open	Negative	7.2-7.8	Extrapolated	[60]
Iceland spar	EPM	Formation water	Calcite/water	24	N/A	Closed	Positive	N/A	Direct	[47]
		Seawater (SW)			N/A		Negative	7.5		
		25 times diluted SW			9.2		Negative	8.5		
Synthetic calcite	EPM	$1x10^{-2}$, $5x10^{-2}$, $1.5x10^{-1}$M NaCl	Calcite/water /air	N/A	N/A	Open	Positive	N/A	N/A	[21]
Synthetic calcite	EPM	10^{-2}M NaCl	Calcite/water	10	9.1	Closed	Pos – Neg	10-11	N/A	[63]
Synthetic calcite	SPM	5×10^{-3}M NaCl	Calcite/water	48	9.11-9.87	Closed	Negative	N/A	N/A	[78]
Synthetic calcite	SPM	5×10^{-3}M NaCl/ 10^{-3}M $NaHCO_3$	Calcite/water	48	9.11-9.87	Closed	Negative	N/A	N/A	[78]
Synthetic calcite	SPM	5×10^{-3}M NaCl/ 10^{-3}M $NaHCO_3$/H_2CO_3/$Ca(OH)_2$	Calcite/water	48	9.11-9.87	Closed	Negative	8.9	Extrapolated	[78]
Synthetic calcite	SPM	$5x10^{-4}$M $CaCl_2$	Calcite/water	48	9.11-9.87	Closed	Positive	N/A	N/A	[78]
Synthetic calcite	EPM	10^{-2}M NaCl	Calcite/water	24	10	Closed	Positive	9.6	Direct	[54]
Synthetic calcite	EPM	10^{-3}M KCl	Calcite/water	168	9.8-10	Closed	Negative	N/A	N/A	[12]
Synthetic calcite	EPM	10^{-3}M KCl/10^{-3}M $CaCl_2$	Calcite/water	168	9.8-10	Closed	Negative	N/A	N/A	[12]
Synthetic calcite	EPM	10^{-3}M KCl/10^{-2}M $CaCl_2$	Calcite/water	168	9.8-10	Closed	Positive	N/A	N/A	[12]
Synthetic calcite	EPM	10^{-3}M NaCl	Calcite/water /air	Few	8.6	Closed	Positive	9.8	Direct	[81]
Synthetic calcite	EPM	10^{-3}M NaCl	Calcite/water /air	Few	8.4	Closed	Positive	9.8	Direct	[80]
Synthetic calcite	EPM	$5.56x10^{-3}$M NaCl	Calcite/water /CO_2	1	8-8.5	Open	Positive	N/A	N/A	[18]
Synthetic calcite	EPM	10^{-3}M NaCl	Calcite/water /air	Few	8.3	Closed	Negative	N/A	N/A	[70]

1078 **Table 1a. (continued)**

Material	Method	Background electrolyte	Equilibrium condition	Equilibration time (hr)	Equilibrium pH (pH_{EQ})	Open vs. closed system	Zeta potential at EQ.	pH_{IEP}	IEP determination	Reference
Natural calcite	EPM	$2x10^{-3}$M $NaClO_4$	Calcite/water	0.5	9-10	Closed	Negative	N/A	N/A	[58]
Natural calcite	EPM	$2x10^{-2}$M $NaClO_4$	Calcite/water /air	0.5	8.2	Open	Negative	8.2	Extrapolated	[48]
Natural calcite	EPM	10^{-2}M NaCl	Calcite/water	24	10	Closed	Negative	9.4	Direct	[54]
Natural (biogenetic) calcite	EPM	10^{-3}M KCl	Calcite/water	168	9.8-10	Closed	Negative	N/A	N/A	[12]
Natural calcite	EPM	10^{-3}M NaCl	Calcite/water /air	Few	8.6	Closed	Negative	N/A	N/A	[81]
Natural calcite	EPM	$2x10^{-3}$M $NaNO_3$	Calcite/water /air	2.2	8.3	Open	Negative	7.8	Extrapolated	[53]
Natural calcite	EPM	10^{-3}M NaCl	Calcite/water /air	Few	8.4	Closed	Negative	N/A	N/A	[80]
Natural calcite	EPM	10^{-3}M KNO_3	Calcite/water /air	1	N/A	Open	Negative	N/A	N/A	[69]
Natural carbonate	EPM	Deionized water	Calcite/water	1	N/A	Closed	Negative	5.2-5.8	Extrapolated	[11]
Natural carbonate	EPM	Formation water	Calcite/water	24	N/A	Closed	Positive	N/A	Direct	[47]
		Seawater (SW)			N/A		Negative	9.25		
		25 times diluted SW			9.2		Negative	10.25		

1079

1080 **Table 1b.**

Material Type	Method	Background electrolyte	Equilibrium condition	Equilibration time (hr)	Equilibrium pH (pH_{EQ})	Open vs. closed system	dζ/dpCa	pCa_{IEP}	IEP determination	Reference
Iceland spar	Electro osmosis	$NaCl/Na_2CO_3/CaCl_2$	Calcite/water	2	9	Closed	N/A	3.33	Extrapolated	[16]
Iceland spar	SPM on packed particles	Deionized water (HNO_3/NaOH)	Calcite/water/ air	1440	8.2	Open	N/A	4.25	Extrapolated	[67]
Iceland spar	EPM	0.571M NaCl	Calcite/water	24	N/A	Closed	N/A	1.65-1.75	Extrapolated	[42]
Synthetic calcite	EPM	$1x10^{-2}$,	Calcite/water/	N/A	N/A	Open	-15.2	4.5	Extrapolated	[21]
		$5x10^{-2}$,	air				-12.8			
		$1.5x10^{-1}$M NaCl					-9.3			
Synthetic calcite	SPM	$2x10^{-3}$M NaCl	Calcite/water	48	9.11-9.87	Closed	-12.7	2.02	Extrapolated	[78]
Synthetic calcite	SPM	$2x10^{-3}/10^{-2}$M ($NaCI/NaHCO_3$)	Calcite/water	48	9.11-9.87	Closed	-10.2	1.92	Extrapolated	[78]
Synthetic calcite	SPM	$2x10^{-3}/10^{-2}$M ($NaCl/CaCl_2$)	Calcite/water	48	9.11-9.87	Closed	-10.1	3.4	Extrapolated	[78]
Synthetic calcite	SPM	$2x10^{-3}/10^{-2}$M ($NaCl/H_2CO_3$)	Calcite/water	48	9.11-9.87	Closed	-10.8	4	Extrapolated	[78]
Synthetic calcite	SPM	$2x10^{-3}/10^{-2}/10^{-2}$M ($NaCl/NaHCO3/H_2CO_3$)	Calcite/water	48	9.11-9.87	Closed	-12.9	3.8	Direct	[78]
Synthetic calcite	SPM	$2x10^{-3}/10^{-2}/10^{-2}$M ($NaCl/NaHCO3/Ca(OH)_2$)	Calcite/water	48	9.11-9.87	Closed	-12.2	3.8	Direct	[78]
Synthetic calcite	EPM	10^{-2}M NaCl	Calcite/water	24	10	Closed	N/A	3.3	Direct	[54]
Synthetic calcite	SPM	10^{-5} – 0.01M $CaCl_2$	Calcite/water	120	9.3-9.9	Closed	-8.34	4.38	Extrapolated	[33]
Synthetic calcite	EPM	10^{-3}M KCl	Calcite/water	168	9.8-10	Closed	-14.5 (in the vicinity of IEP)	2.7	Direct	[12]
Natural calcite	EPM	10^{-2}M NaCl	Calcite/water	24	10	Closed	N/A	4	Direct	[54]
Stevns Klint chalk	EPM	$CaCl_2$ and $NaSO_4$ in 0.571M NaCl	Chalk/water/air	48	Controlled at 8.4	Closed	N/A	N/A	N/A	[88]
Natural carbonate	EPM	Deionized water (DI)	Calcite/water	1	Controlled at 8.4	Closed	N/A	0.2-0.75	Extrapolated	[11]
Natural carbonate	SPM in intact samples	0.05M NaCl	Calcite/water/	168-720	8.2	Closed	-5.29	0.61	Direct	[4]
		0.5M NaCl	air				-4.35	0.49		
		2M NaCl					-2.75	0.41		

1081

Table 2: Properties and mineralogy of rock samples used in this study compared to Portland used by *Alroudhan et al. [4]***.**

Property/rock	**Ketton**	**Estaillades**	**Portland**
Description	Middle Jurassic Oolitic limestone from UK	Upper Cretaceous limestone from France	Upper Jurassic Ooparite limestone from UK
Porosity	23% ±0.5	28% ±0.5	20% ±0.5
Permeability	1.4 Darcy ±0.4	0.13 Darcy ±0.2	0.005 Darcy ±0.001
Intrinsic Formation Factor (*F*)	13.87 ±0.5	12.92 ±0.5	22.04 ±0.5
Compositions	97% calcite ($CaCO_3$)	97% calcite ($CaCO_3$)	96.6% calcite ($CaCO_3$)
	3% magnesium*	3% magnesium*	3.4% quartz
Dimensions	Length (L) =0.076 m	Length (L) =0.076 m	Length (L) =0.076 m
	Diameter (D) =0.038 m	Diameter (D) =0.038 m	Diameter (D) =0.038 m

***Magnesium (Mg^{2+}) is likely incorporated into the calcite structure as $MgCO_3$ or $CaMg(CO_3)_2$**

Figure Captions

Figure 1: (a) A schematic representation of the electrical double layer at the calcite-water interface. The surface speciation sites (>CO_3H^0, >CaO^{-+}, >CO_3Ca^+, >$CaOH^0$, >$CaCO_3^-$, $CaOH_2^+$ and >CO_3^-) are from [*57*]. The Stern layer is described by three planes. The 0-plane (x=0) corresponds to the hydrolysis layer where H and OH are chemi-bonded to the bulk ions [*71*]. The 1-plane (x=1) denotes inner-sphere complexes and corresponds to the inner Helmholtz plane (IHP), while the 2-plane (x=2) denotes outer-sphere complexes and corresponds to the outer Helmholtz plane (OHP; [*85*]). (b) A schematic representation of the variation in the electrical potential with distance from the mineral surface. Here the mineral surface is negatively charged, consistent with the surface complexation model of [*29*], but the zeta potential is positive because of adsorption of the lattice PDIs Ca^{2+} and CO_3^{2-}.

Figure 2: Zeta potential of (a) Iceland spar and synthetic calcite and (b) natural calcite and carbonate rocks in indifferent electrolytes as a function of pH. Measurements were obtained using the electrophoretic mobility method (EPM), with the exception of *Somasundaran and Agar [67]* (diamonds) and *Thompson and Pownall [78]* (squares). Error bars are shown when reported by the source.

In (a), data from *Somasundaran and Agar [67]* in deionized water after different mixing times (♦: no mixing; ◊: after 1 week; ◇: after two months of mixing); *Sampat Kumar et al. [60]* in deionised water (+); *Siffert and Fimbel [63]* in 10^{-2}M NaCl electrolyte (∗: mass dispersed = 50 mg; grey ∗: 30 mg); *Thompson and Pownall [78]* in various electrolytes (■: NaCl (5×10^{-3}M); □: NaCl (5×10^{-3}M)/$NaHCO_3$ (1×10^{-3}M); ☐: NaCl (5×10^{-3}M)/$NaHCO_3$ (1×10^{-3}M)/H_2CO_3/$Ca(OH)_2$); *Cicerone et al. [12]* in 10^{-3}M KCl electrolyte (▲); *Vdović and Bišćan [81]* in 10^{-3}M NaCl electrolyte (○); *Vdovic [80]* in 10^{-3}M NaCl electrolyte (●); *Eriksson et al. [18]* in 5.56×10^{-3}M NaCl electrolyte (×); *Sondi et al. [70]* in 10^{-3}M NaCl electrolyte (△) and *Kasha et al. [42]* in deionized water (○). Grey symbols show data from *Mahani et al. [47]* in various electrolytes (▲: formation brine; ♦: seawater; ■: 25 times diluted seawater).

In (b), data from *Mishra [48]* in $2x10^{-2}$M $NaClO_4$ electrolyte (+); *Rao et al. [58]* in $2x10^{-3}$M $NaClO_4$ electrolyte (♦); *Cicerone et al. [12]* in 10^{-3}M KCl electrolyte (△); *Vdović and Bišćan [81]* in 10^{-3}M NaCl electrolyte (◊); [*53*] in $2x10^{-3}$M $NaNO_3$ electrolyte (∗); *Vdovic [80]* in 10^{-3}M NaCl electrolyte (○: limestone; ●: lake sediment) and *Somasundaran et al. [69]* in 10^{-3}M KNO_3 electrolyte (■). Grey symbols show data on natural carbonate rocks in various electrolytes (●: deionized water containing 0.09 M $CaCl_2$ from [*11*]; ▲: formation brine; ♦: seawater; ■: 25 times diluted seawater, all from [*47*]).

Figure 3: Zeta potential and electrophoretic mobility of synthetic calcite and Iceland spar as a function of pH in experiments with (a) constant pCa and (b) controlled pCO_2. Error bars are shown when reported by the source.

In (a), all data are from synthetic calcite. Data from *Foxall et al. [21]* **in 10^{-2}M NaCl electrolyte with pCa = 2.1 (□); *Thompson and Pownall [78]* in $5x10^{-4}$M $CaCl_2$ electrolyte with pCa = 3.3 (×); *Cicerone et al. [12]* in 10^{-3}M KCl electrolyte with pCa = 2 (△) and pCa = 3 (◇), and *Sondi et al. [70]* in 10^{-3}M NaCl electrolyte with pCa = 2 (○).**

In (b), all data are from powdered Iceland spar in deionized water with various pCO_2. Data from *Moulin and Roques [51]* **(◆: pCO_2 = 0.023; ◇: pCO_2 = 0.234) and** *Heberling et al. [29]* **(△: pCO_2 = 1; ○: $pCO_2 = 10^{-3.44}$; □: $pCO_2 = 10^{-5.2}$).**

Figure 4: Zeta potential of synthetic calcite and natural carbonate in indifferent electrolytes as a function of pCa, at (a) low Ca concentration only and (b) low to high Ca concentration. Error bars are shown when reported by the source.

In (a), all data are from powdered synthetic calcite with the exception of *Alroudhan et al. [4]* **(grey symbols). Data from** *Thompson and Pownall [78]* **in different aqueous compositions (■: NaCl ($2x10^{-3}$M)/$NaHCO_3$ (10^{-2}M); □: NaCl ($2x10^{-3}$); ☐: NaCl ($2x10^{-3}$M)/$NaHCO_3$ (10^{-2}M)/$Ca(OH)_2$ (10^{-2}M); ■: NaCl ($2x10^{-3}$M)/$NaHCO_3$ (10^{-2}M)/H_2CO_3 (10^{-2}M)); *Foxall et al. [21]* in three different NaCl concentrations (▲: $1x10^{-2}$M; △: $5x10^{-2}$M; big △: $1.5x10^{-1}$M); *Huang et al. [33]* in 0.01 $CaCl_2$ electrolyte (×) and *Cicerone et al. [12]* in 10^{-3}M KCl electrolyte (○). Grey diamonds show data from *Alroudhan et al. [4]* on natural carbonate in 0.05M NaCl electrolyte at high pCa (♦: SPM data; ◊: EPM data); the full span of these data is shown in Figure 2b.**

In (b), all data are from natural calcite and carbonate rocks, with the exception of *Kasha et al. [42]* **(filled symbols). Data from** *Zhang and Austad [88]* **on powdered Stevns Klint chalk in 0.571M NaCl electrolyte (×);** *Chen et al. [11]* **in deionized water (○);** *Kasha et al. [42]* **in synthesized brines equivalent to seawater composition (●) and** *Alroudhan et al. [4]* **in 0.05M NaCl (◊). Grey symbols show data from** *Alroudhan et al. [4]* **in intact natural carbonate rocks in various NaCl concentrations (♦: 0.05M;▲: 0.5M; ■: 2M; all from; error bars are the same size or smaller than the symbols).**

Figure 5: Zeta potential of synthetic calcite and natural carbonate as a function of (a) pMg and (b) pSO_4. Error bars are shown when reported by the source.

In (a), open symbols show zeta potential as a function of pMg. Data from *De Groot and Duyvis [14]* in deionized water (△); *Smallwood [64]* in deionized water (□); *Zhang et al. [87]* in 0.571M NaCl electrolyte (×); *Chen et al. [11]* in deionized water (○) and *Alroudhan et al. [4]* in intact natural Portland carbonate in 0.05M NaCl electrolyte (◇; error bars for these data are the same size or smaller than the symbols). For comparison, filled symbols show measurements as a function of pCa when available from the same studies.

In (b), data from *Smallwood [64]* on synthetic calcite in deionized water (□); *Zhang and Austad [88]* on Stevns Klint chalk in 0.571M NaCl electrolyte (×) and *Alroudhan et al. [4]* in intact natural Portland carbonate in various NaCl electrolytes (◆: 0.05M; ◇: 0.5M; error bars are the same size or smaller than the symbols; data from).

Figure 6: Calcite-water-CO_2 equilibrium. Plot (a) shows calcium concentration (expressed as pCa) and pH measured as a function of time during equilibration of natural Portland rock samples with deionised water. Plot (b) shows carbonate speciation into H_2CO_3, HCO_3^-, and CO_3^{2-} as a function of pH. Modified from *Alroudhan et al. [4]*.

Figure 7: (a) Effect of NaCl concentration on zeta potential on the Ketton (squares) and Estaillades (triangles) samples. Data obtained on the Portland carbonate sample by *Alroudhan et al. [4]* are shown for comparison (grey diamonds). The inset plots (b) and (c) show typical example measurements of voltage and pressure against time from the SPM used to determine the zeta potential. When pressure and voltage respond in the same sense the zeta potential is positive and *vice-versa*. The polarity of the zeta potential is accurately determined even when its value is close to zero.

Figure 8: Zeta potential versus (a) pCa and pMg, and (b) pSO_4 for the Ketton (squares) and Estaillades (triangles and circles) samples at different NaCl concentrations. Data obtained on the Portland carbonate sample by *Alroudhan et al. [4]* **are shown for comparison (diamonds).**

Figure 9: (a) Relationship between pH and pCa or pMg obtained from all the experiments shown in Figure 8, along with linear regressions to the data. (b) Data shown in Figure 8 replotted against pH using the linear regression shown in (a).

Figure 10: Equilibrium pCa (a) and pSO_4 (b) versus NaCl concentration for the Ketton (squares) and Estaillades (triangles) samples. Data obtained on the Portland carbonate sample by Alroudhan et al. [4**] are shown for comparison (diamonds).**

Figure 11: Impact of pSO_4 on pCa and zeta potential measured on the Estaillades sample. (a) pCa measured during the experiments shown in Figure 8b in which SO_4^{2-} was added to pre-equilibrated NaCl brine plotted against measured pSO_4. (b) Zeta potential from the experiments shown in Figure 8b plotted against the measured pCa recorded in (a).

1170 **Figures**

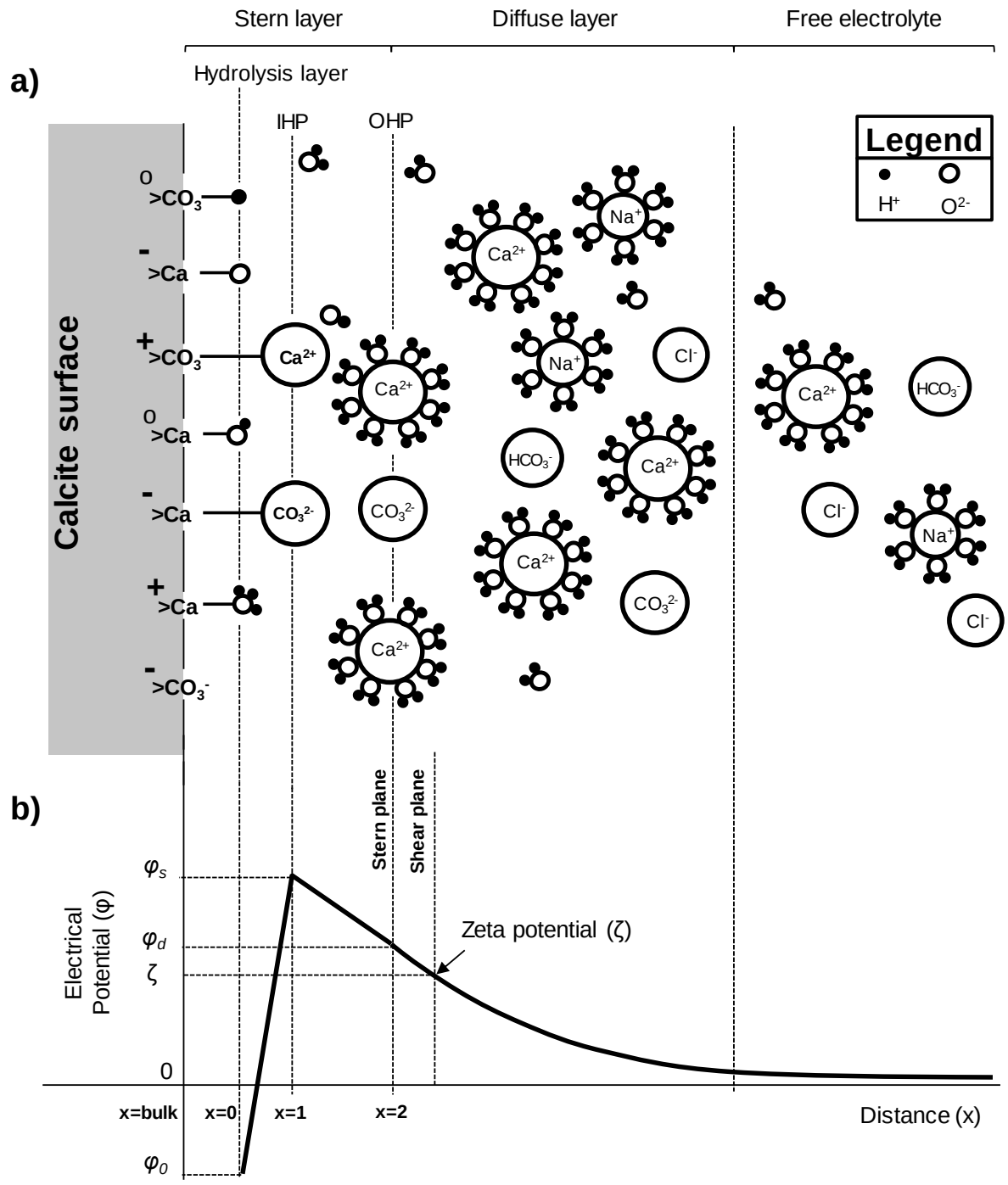

1171

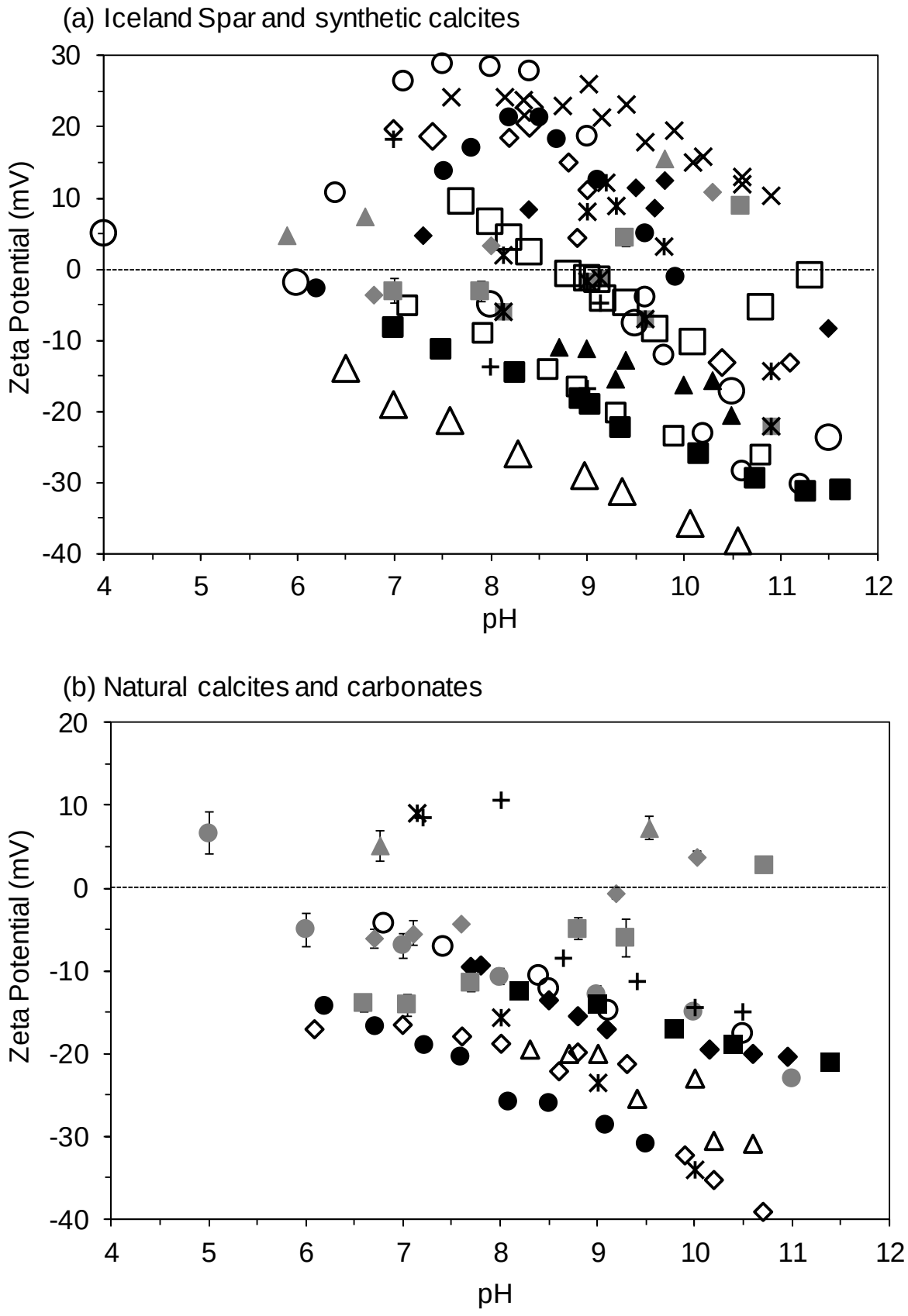
(a) Iceland Spar and synthetic calcites
Zeta Potential (mV)
pH
30
20
10
0
-10
-20
-30
-40
4
5
6
7
8
9
10
11
12
(b) Natural calcites and carbonates
Zeta Potential (mV)
pH
20
10
0
-10
-20
-30
-40
4
5
6
7
8
9
10
11
12

1172

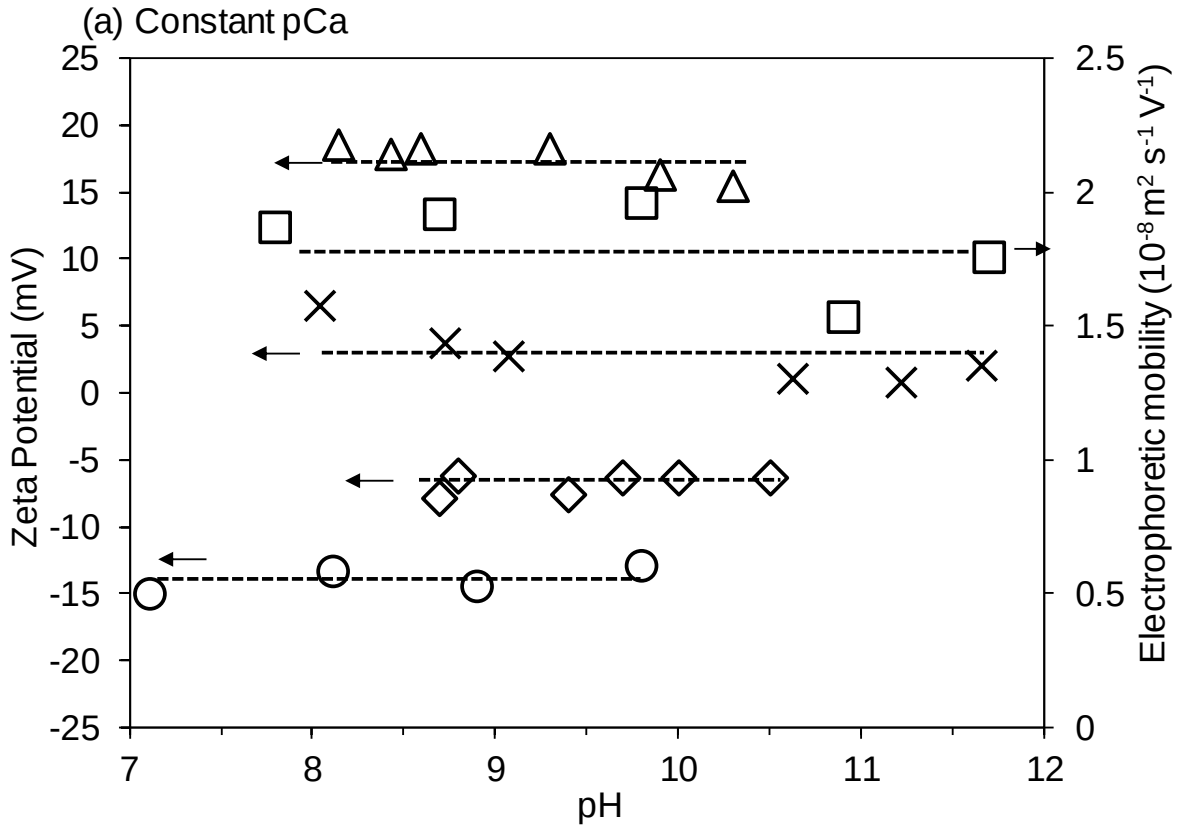
(a) Constant pCa
Zeta Potential (mV)
Electrophoretic mobility (10^{-8} m^2 s^{-1} V^{-1})
pH

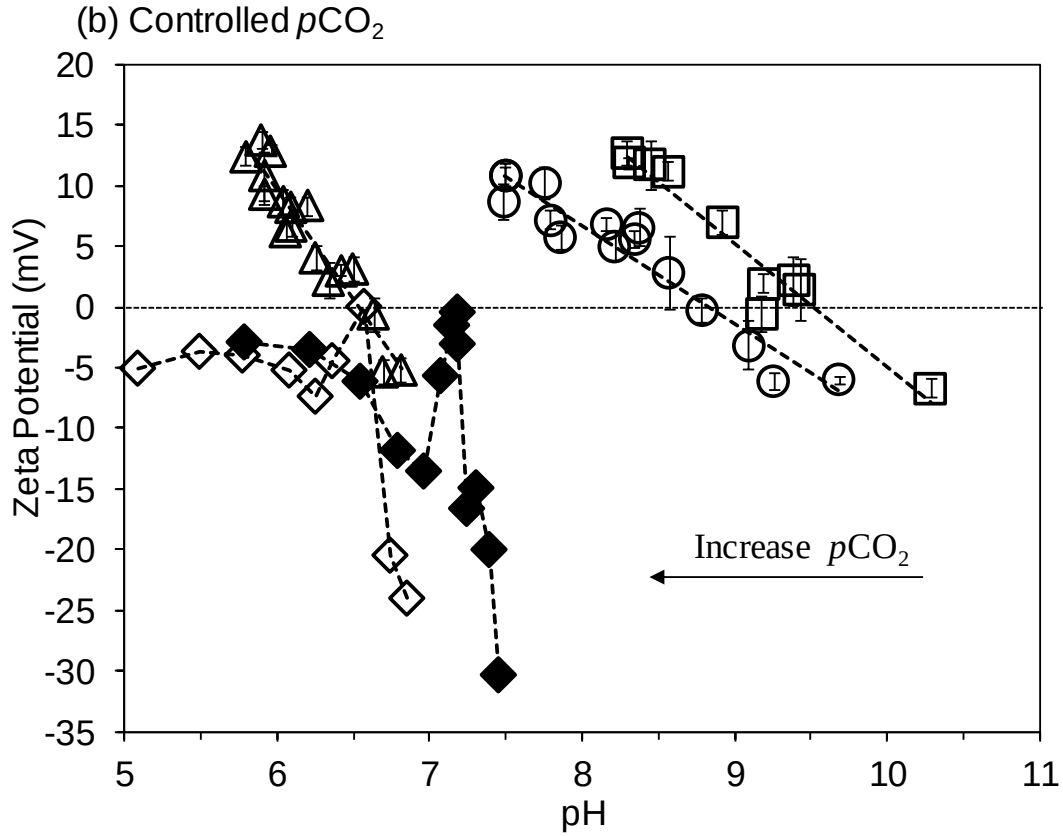
(b) Controlled pCO_2
Zeta Potential (mV)
Increase pCO_2
pH

1173

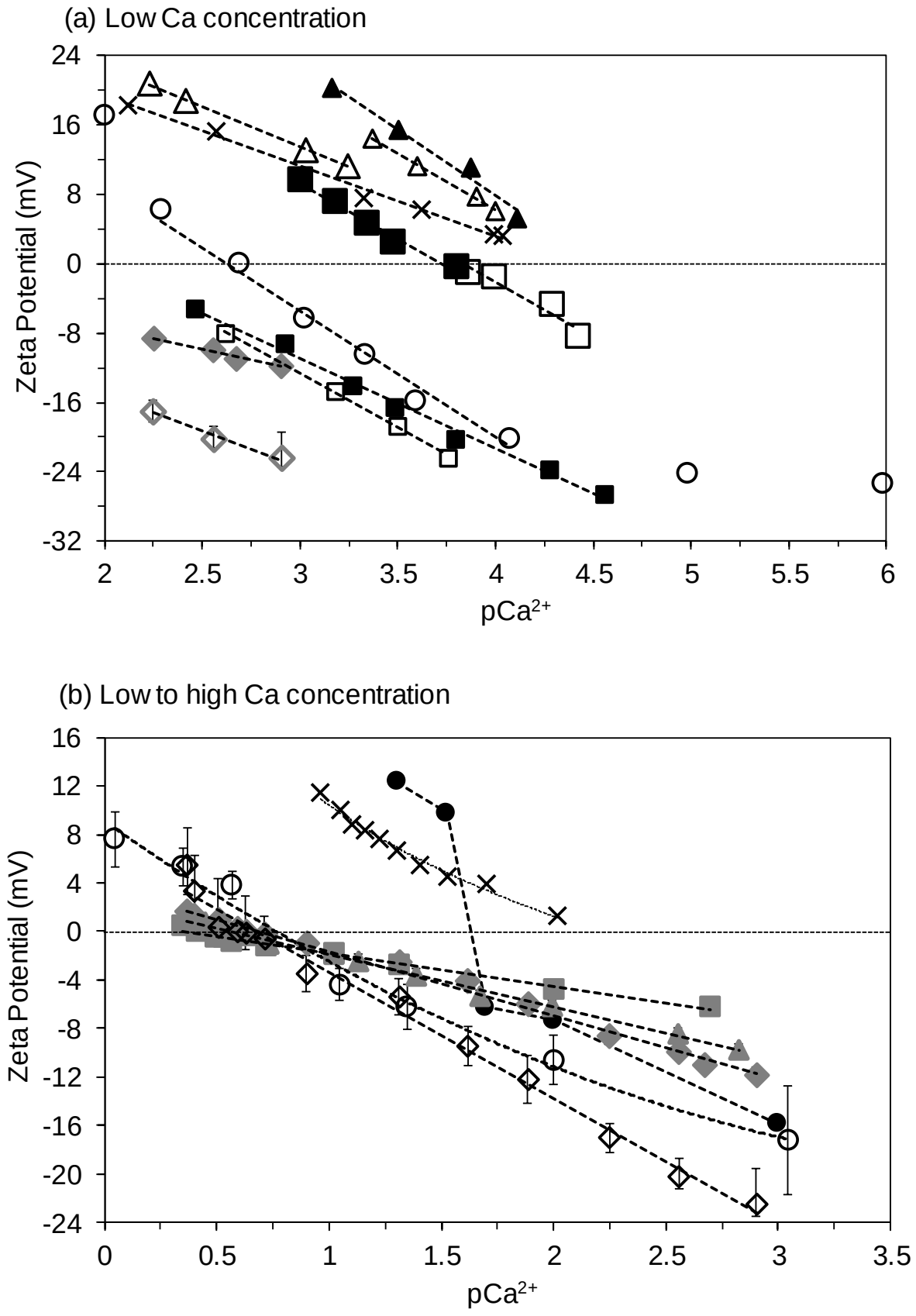
(a) Low Ca concentration
Zeta Potential (mV)
24
16
8
0
-8
-16
-24
-32
2
2.5
3
3.5
4
4.5
5
5.5
6
pCa2+
(b) Low to high Ca concentration
Zeta Potential (mV)
16
12
8
4
0
-4
-8
-12
-16
-20
-24
0
0.5
1
1.5
2
2.5
3
3.5
pCa2+

1174

(a) Effect of Mg on zeta potential of calcite

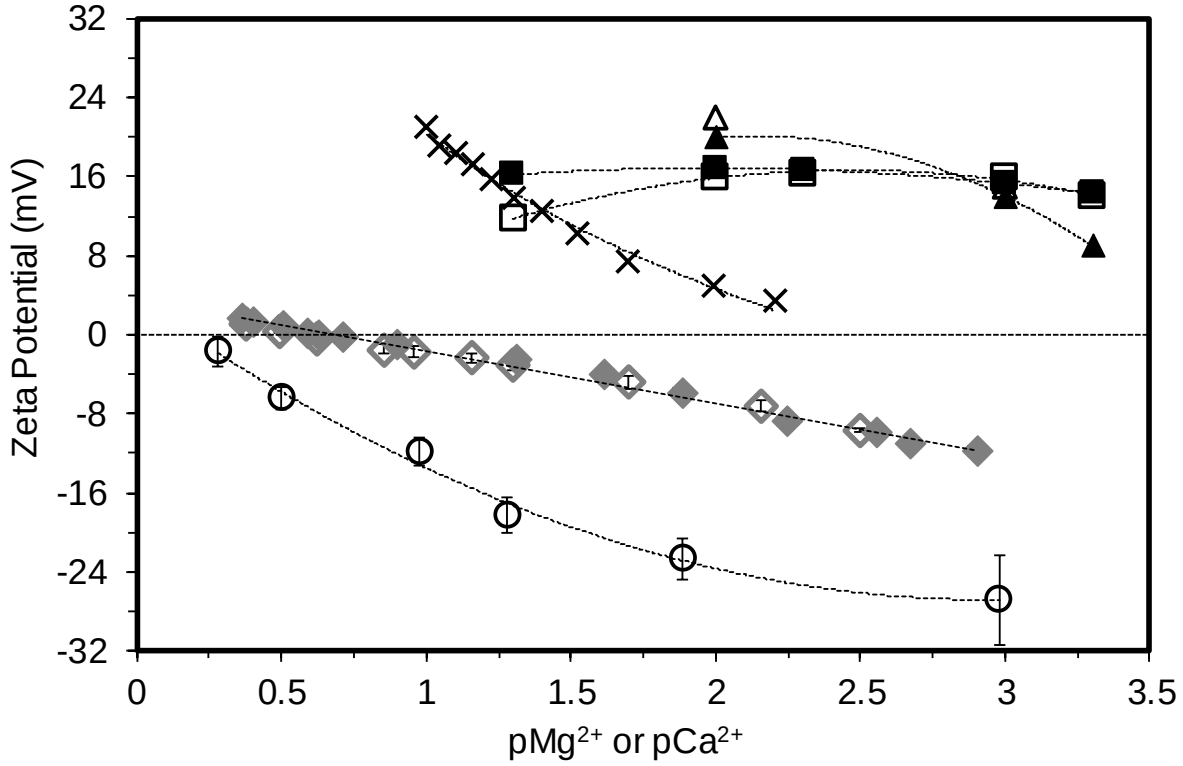

(b) Effect of SO_4 on zeta potential of calcite

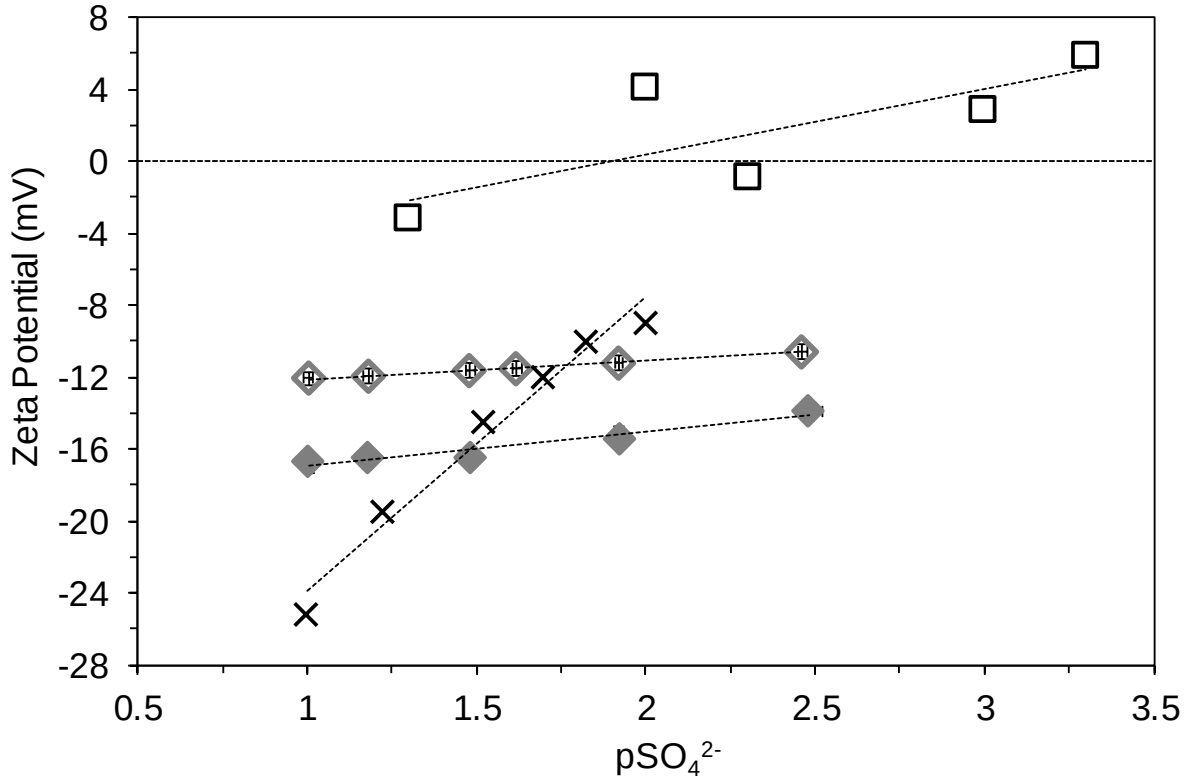

1175

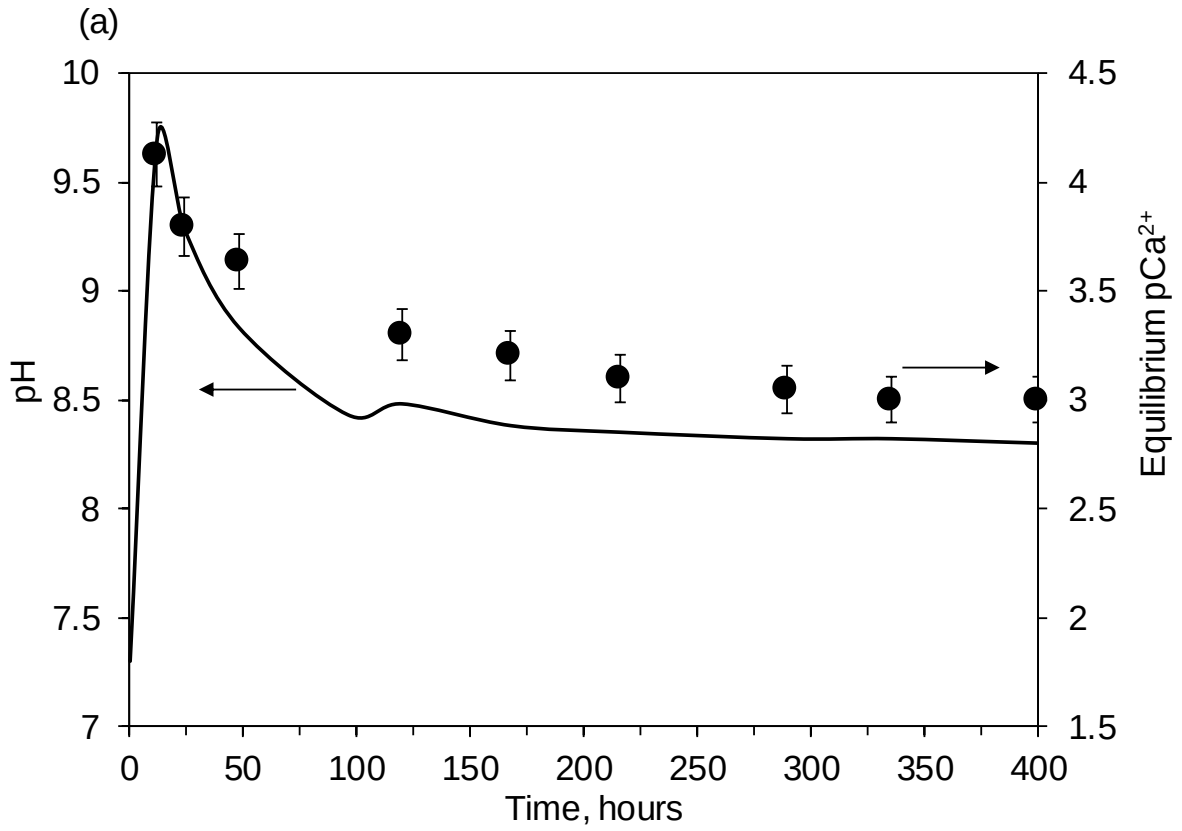
(a)
10
9.5
9
8.5
8
7.5
7
pH
4.5
4
3.5
3
2.5
2
1.5
Equilibrium pCa2+
0
50
100
150
200
250
300
350
400
Time, hours

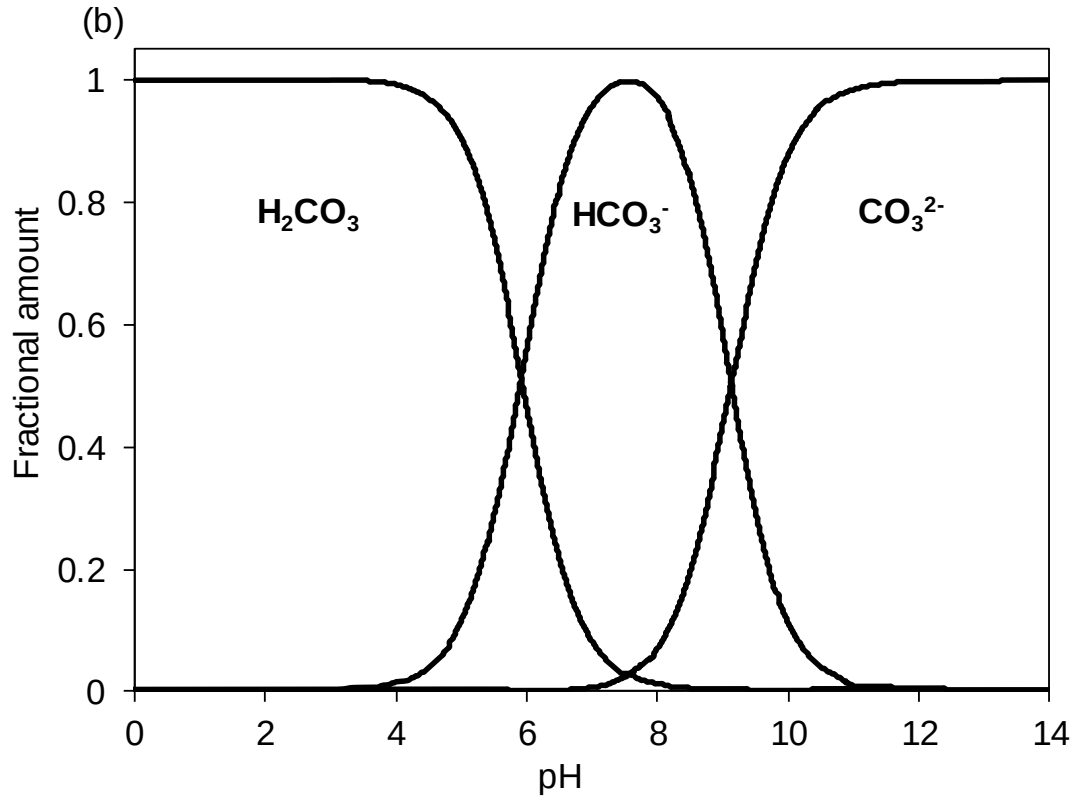
(b)
1
0.8
0.6
0.4
0.2
0
Fractional amount
H2CO3
HCO3-
CO32-
0
2
4
6
8
10
12
14
pH

1176

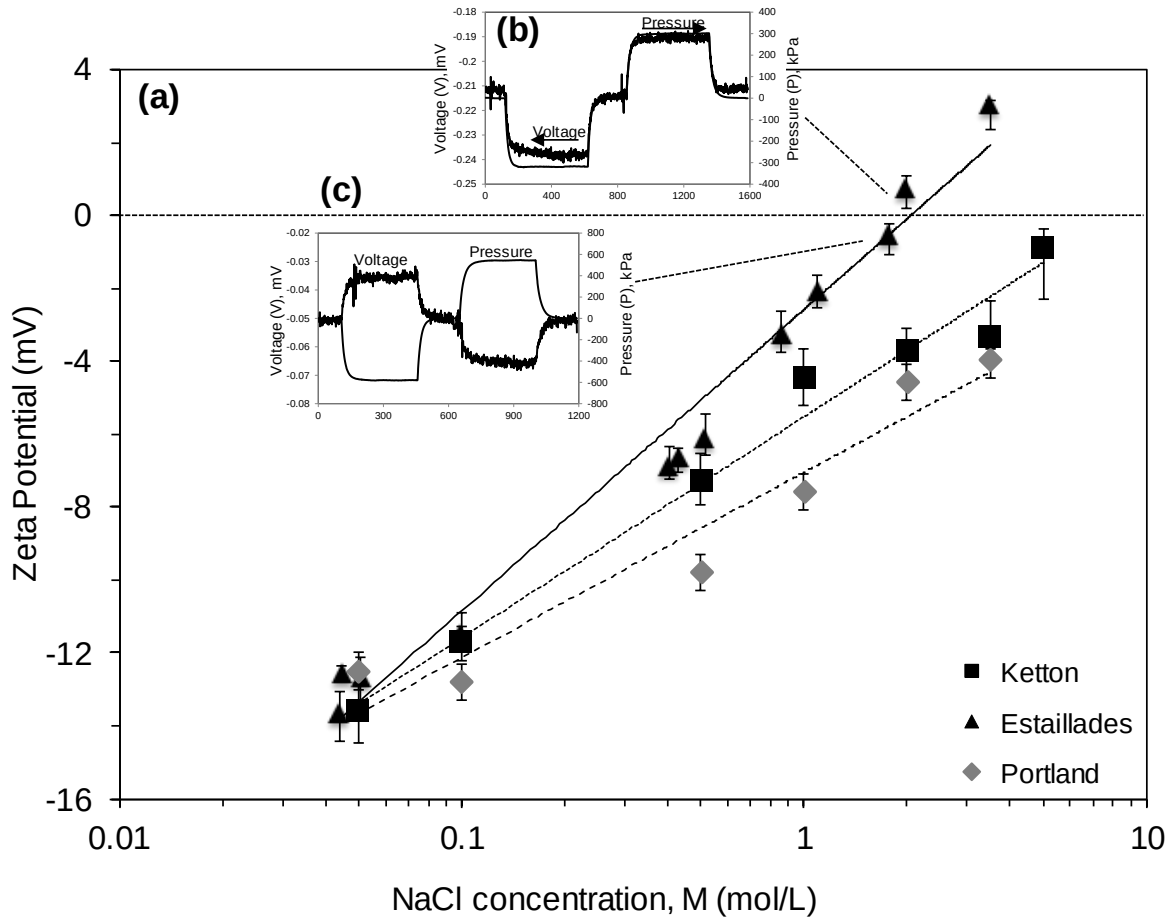
(a)
(b)
(c)
Pressure
Voltage
Voltage (V), mV
Pressure (P), kPa
Zeta Potential (mV)
NaCl concentration, M (mol/L)
Ketton
Estaillades
Portland

1177

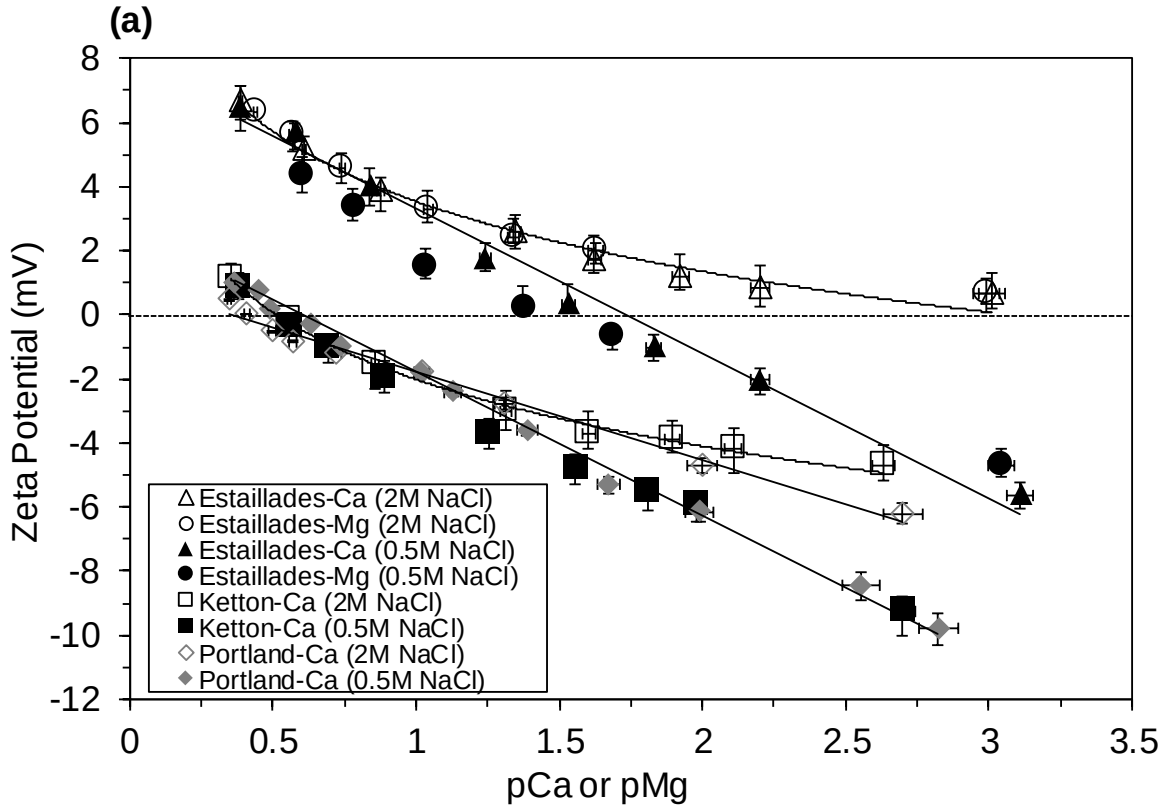
(a)
Zeta Potential (mV)
pCa or pMg
Estaillades-Ca (2M NaCl)
Estaillades-Mg (2M NaCl)
Estaillades-Ca (0.5M NaCl)
Estaillades-Mg (0.5M NaCl)
Ketton-Ca (2M NaCl)
Ketton-Ca (0.5M NaCl)
Portland-Ca (2M NaCl)
Portland-Ca (0.5M NaCl)

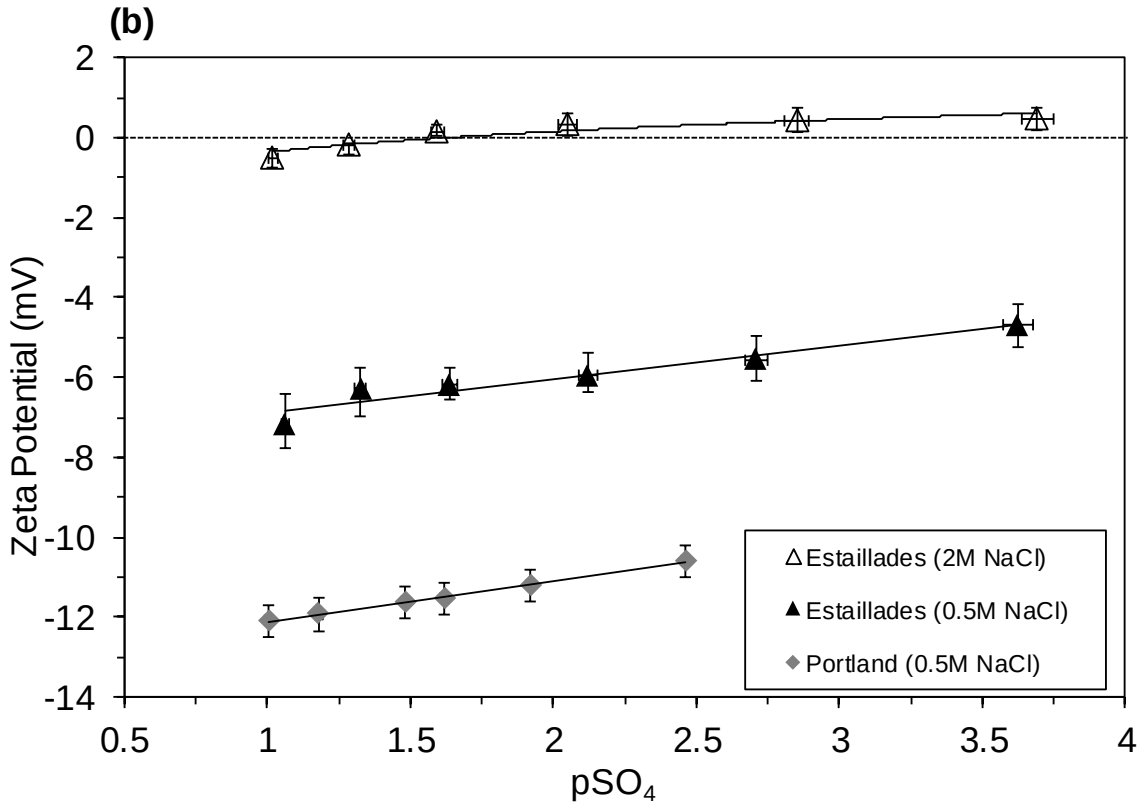
(b)
Zeta Potential (mV)
pSO4
Estaillades (2M NaCl)
Estaillades (0.5M NaCl)
Portland (0.5M NaCl)

1178

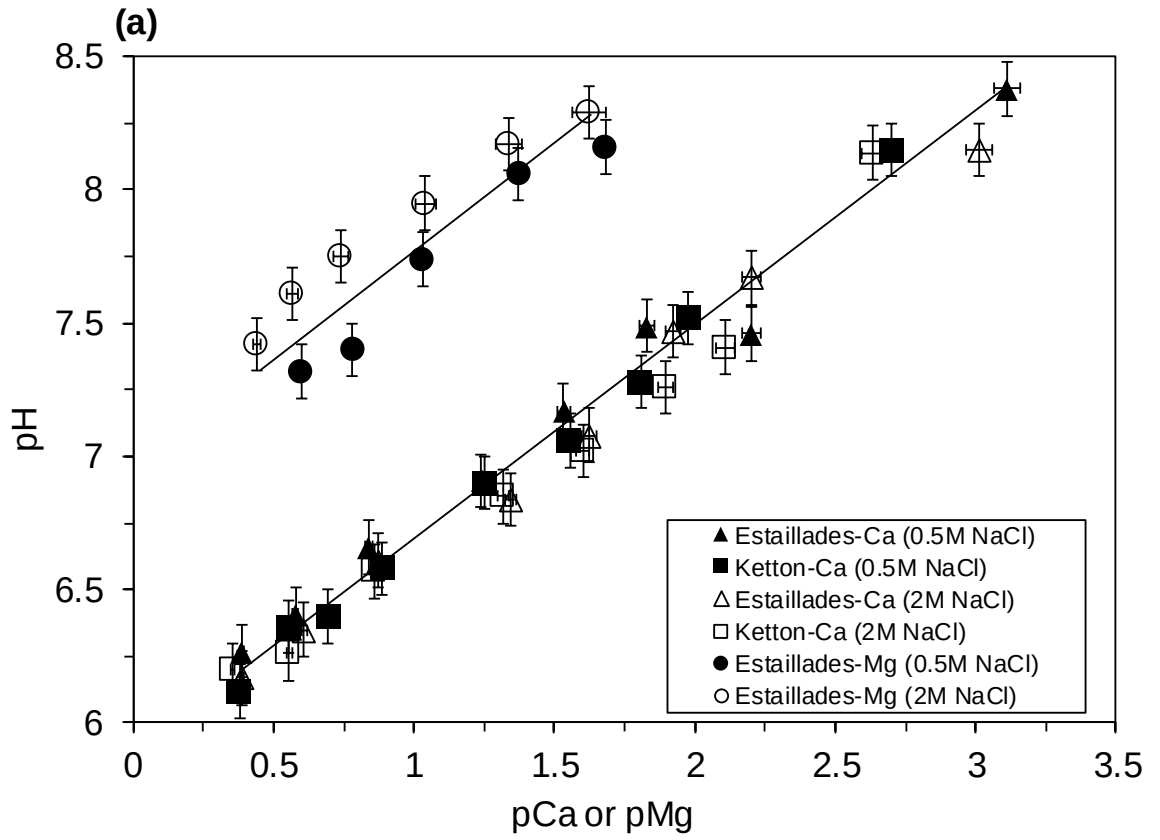
(a)
pH
pCa or pMg
Estaillades-Ca (0.5M NaCl)
Ketton-Ca (0.5M NaCl)
Estaillades-Ca (2M NaCl)
Ketton-Ca (2M NaCl)
Estaillades-Mg (0.5M NaCl)
Estaillades-Mg (2M NaCl)

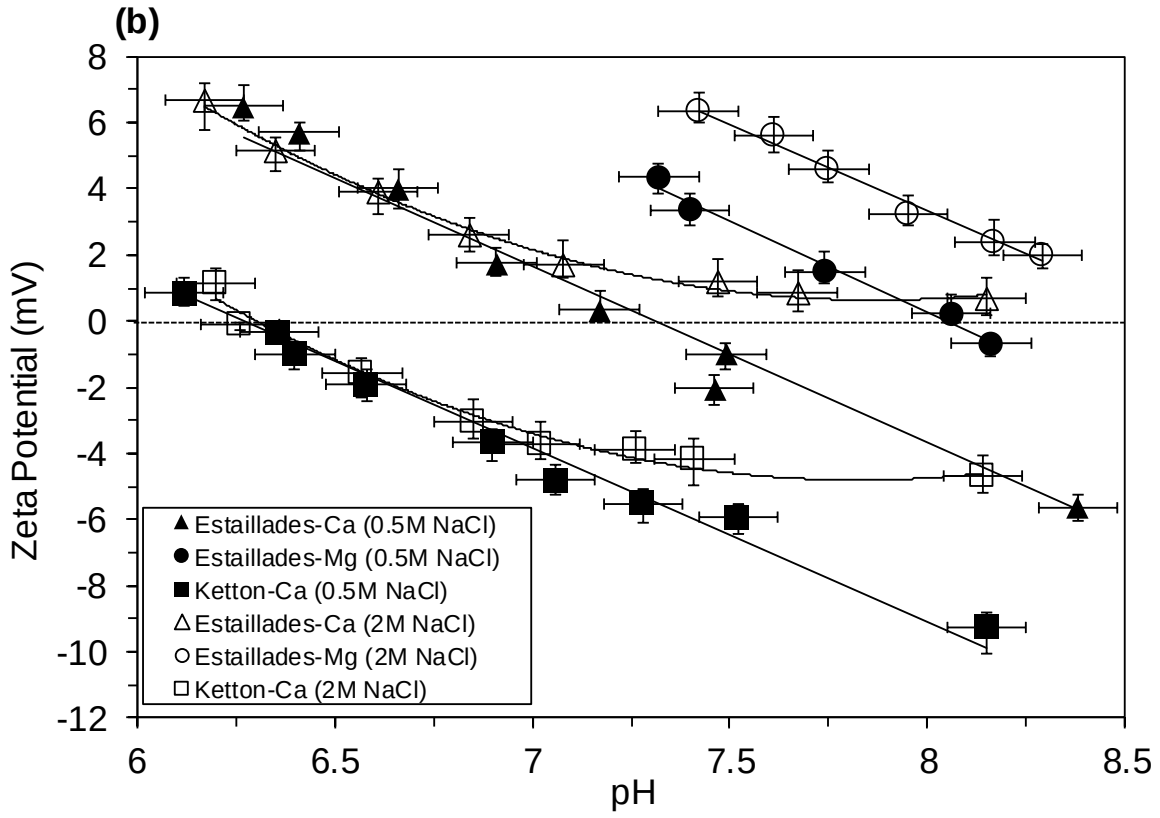
(b)
Zeta Potential (mV)
pH
Estaillades-Ca (0.5M NaCl)
Estaillades-Mg (0.5M NaCl)
Ketton-Ca (0.5M NaCl)
Estaillades-Ca (2M NaCl)
Estaillades-Mg (2M NaCl)
Ketton-Ca (2M NaCl)

1179

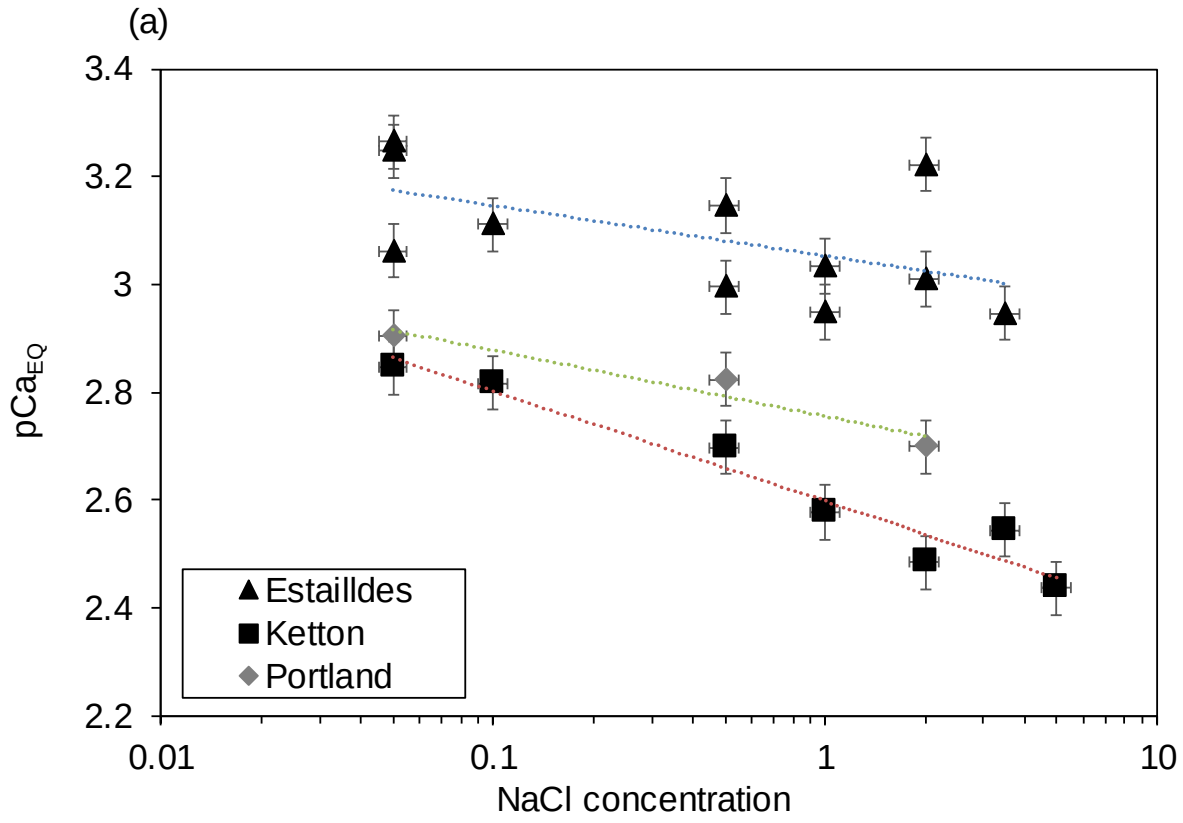
(a)
3.4
3.2
3
2.8
2.6
2.4
2.2
pCa_EQ
0.01
0.1
1
10
NaCl concentration
Estailldes
Ketton
Portland

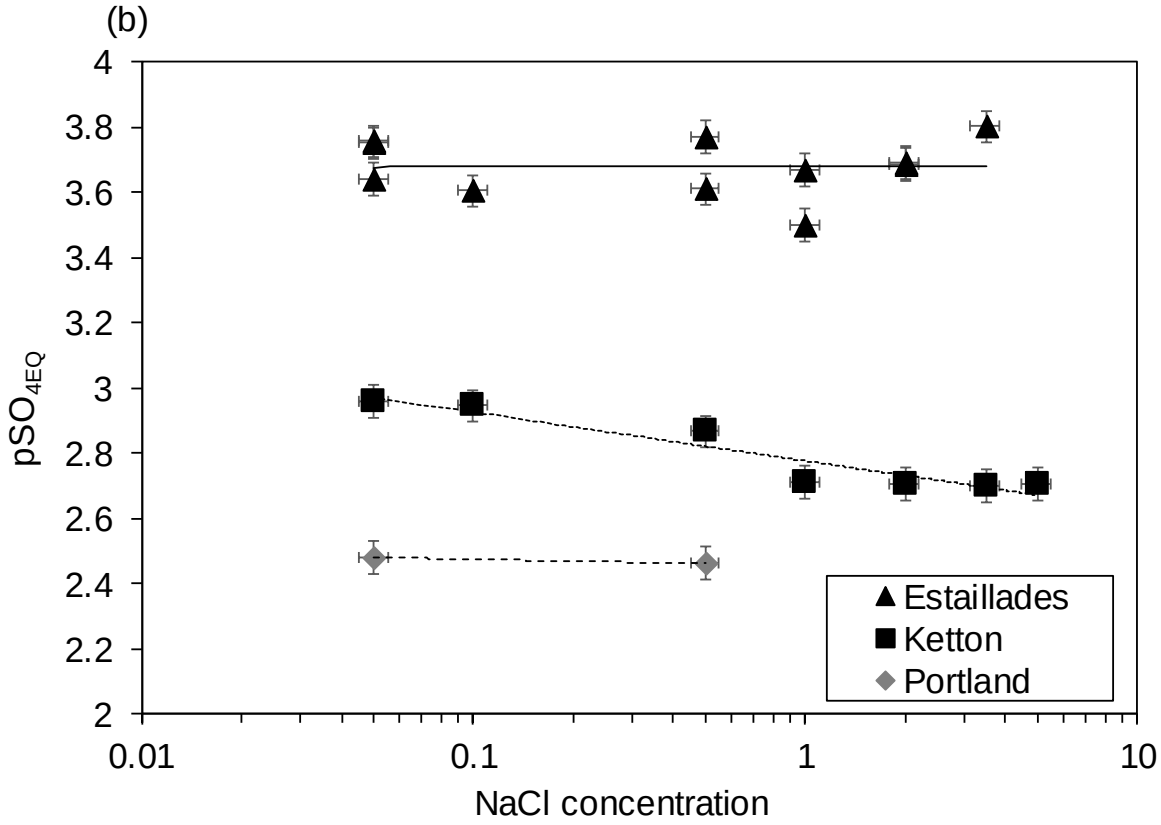
(b)
4
3.8
3.6
3.4
3.2
3
2.8
2.6
2.4
2.2
2
pSO_4EQ
0.01
0.1
1
10
NaCl concentration
Estaillades
Ketton
Portland

1180

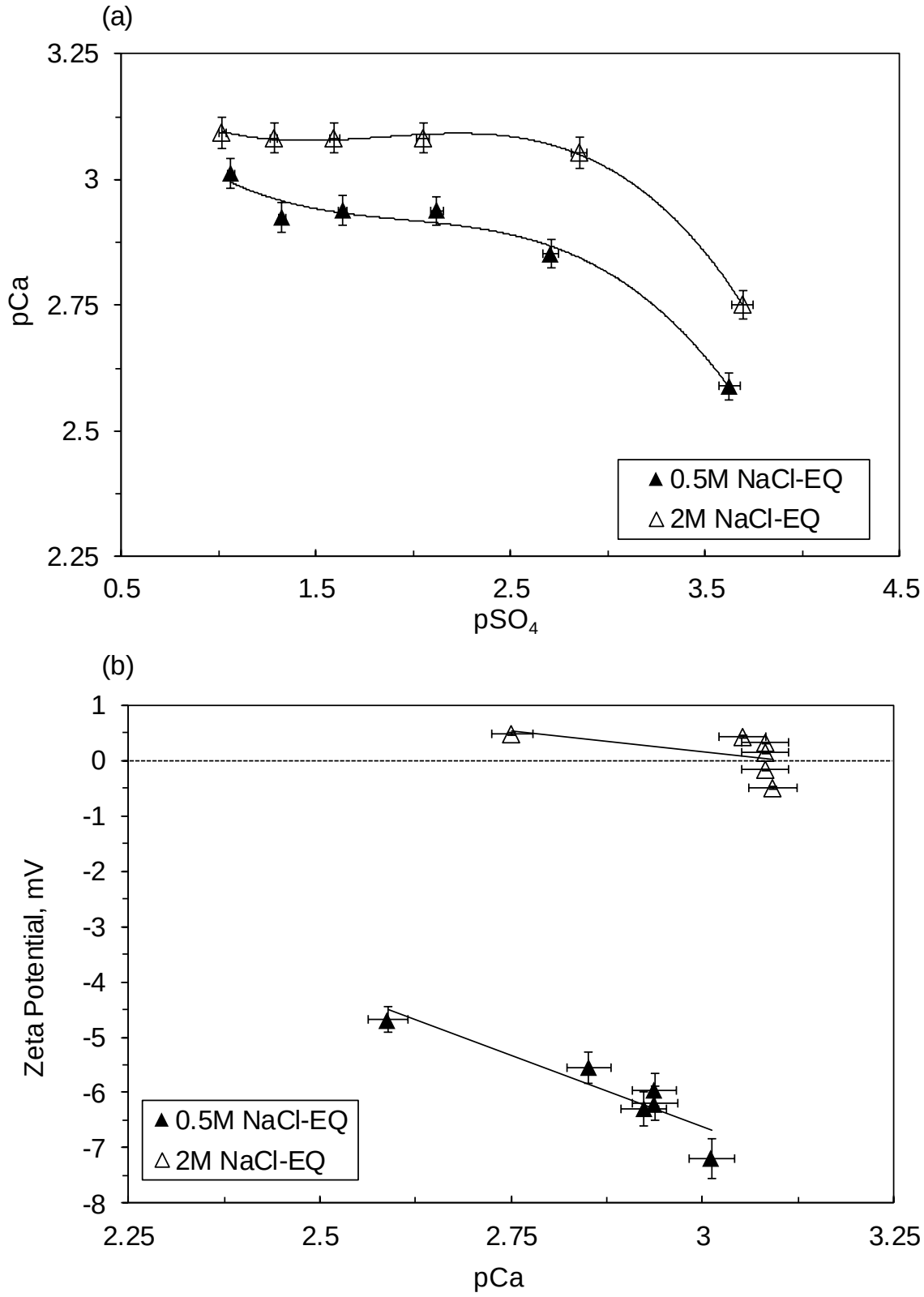
(a)
3.25
3
2.75
2.5
2.25
pCa
0.5
1.5
2.5
3.5
4.5
pSO4
▲ 0.5M NaCl-EQ
△ 2M NaCl-EQ
(b)
1
0
-1
-2
-3
-4
-5
-6
-7
-8
Zeta Potential, mV
2.25
2.5
2.75
3
3.25
pCa
▲ 0.5M NaCl-EQ
△ 2M NaCl-EQ

1181